



**UNIVERSITY of the  
WESTERN CAPE**

**Diagnostic accuracy of maxillary periapical pathology perforating the sinus floor:  
a comparison of pantomograph and CBCT images**



Jaco Walters

*A mini-thesis submitted in partial fulfilment of the requirements for the degree Magister  
Scientiae in the Department of Diagnostics and Radiology, Faculty of Dentistry,  
University of the Western Cape.*

July 2020

Supervisor: Dr S. Shaik  
Co-supervisor: Dr N. Behardien

<http://etd.uwc.ac.za/>

## KEYWORDS

Apical periodontitis

Cone-beam computed tomography

Dentistry

Diagnostic accuracy

Maxillary sinus

Maxillofacial

Oral pathology

Pantomograph

Perforation

Radiology



## ABSTRACT

**Introduction:** Periapical lesions are fairly common pathology associated with the apex of a non-vital tooth. Some chronic lesions develop without an acute phase with no recollection of previous symptoms. It is known that maxillary odontogenic infections can breach the sinus floor with succeeding complications. Pantomography, a widespread conventional radiographic technique, provides a generalized view of the maxillofacial region. Advanced modalities like CBCT may facilitate in navigating complex anatomy, which would otherwise be obscured.

**Aim:** To evaluate the diagnostic accuracy of PAN and CBCT images related to maxillary posterior teeth periapical pathology that perforates the floor of the maxillary sinus by comparing two radiographic modalities.

**Material and methods:** Data from archived CBCT volumes and corresponding conventional PAN images of subjects were examined. The presence and radiographic features of the pathology was recorded for both modalities. A comparison was made by cross-examination.

**Results:** 42 cases of maxillary sinus floor perforation of odontogenic origin were analysed. Median and average age showed prevalence for the 4<sup>th</sup> decade with a negligible gender ratio. Majority of cases associated the 1<sup>st</sup> molar with slight 2<sup>nd</sup> quadrant predominance. Greater number of lesions presented asymptomatic. Predominant radiographic features included well-defined lucent/low-densities. More than half of the associated teeth were previously restored or endodontically treated. Almost all cases depicted maxillary sinus mucosal reaction. The overall performance of the PAN appeared 'poor' and insufficient as a diagnostic tool in detecting a perforation.

**Conclusion:** High rates of asymptomatic lesions were on restored or endodontically treated teeth. Inconclusive clinical examination, testing, and conventional imaging of a suspicious tooth may prompt further investigation. In selected cases, small FOV CBCT accompanied by appropriate interpretation and reporting thereof by a skilled clinician may be considered. A subsequent correct diagnosis and treatment plan can facilitate achieving an uncomplicated outcome.

## DECLARATION

I declare that *Diagnostic accuracy of maxillary periapical pathology perforating the sinus floor: a comparison of pantomograph and CBCT images* is my own work, that it has not been submitted before for any degree or examination in any other university, and that all the sources I have used or quoted have been indicated and acknowledged as complete references.

Jaco Walters

July 2020

Signed: .....



## ACKNOWLEDGEMENTS

I would like to express my sincere thanks and appreciation to the following people for their respective contributions during this study:

- my supervisor Dr Shoayeb Shaik,
- my co-supervisor Dr Nashreen Behardien,
- the staff, and colleagues at the Department of Diagnostics and Radiology,
- Dr Paul Botha,
- my friends,
- and family.



## DEDICATION

*This text is dedicated to my grandmother Johanna Catharina 'Joan' van der Merwe (née Groenewald) b. 20<sup>th</sup> Jan. 1931 an inspiring individual who, in spite of life's curveballs, maintains a lifelong unwavering lust for knowledge and personal development.*

*'Dankie ouma'*



## TABLE OF CONTENT

KEYWORDS .....	ii
ABSTRACT .....	iii
DECLARATION .....	iv
ACKNOWLEDGEMENTS .....	v
DEDICATION .....	vi
TABLE OF CONTENT .....	vii-ix
LIST OF TABLES .....	x
LIST OF FIGURES .....	xi
ACRONYMS AND ABBREVIATIONS .....	xii
GLOSSARY .....	xiii-xiv
CHAPTER 1: INTRODUCTION .....	1
CHAPTER 2: LITERATURE REVIEW .....	2-8
2.1. Panoramic Radiography .....	2
2.2. Cone-beam computed tomography .....	3-4
2.3. Periapical pathology .....	4-5
2.4. The maxillary sinus .....	5-6
2.5. Spread of odontogenic infections in the maxillary teeth .....	6-8
2.6. Inference .....	8
CHAPTER 3: AIM AND OBJECTIVES .....	9
3.1. Aim .....	9
3.2. Objectives .....	9
CHAPTER 4: MATERIALS AND METHODS .....	10-14
4.1. Study design .....	10
4.2. Equipment .....	10
4.3. Target population .....	10
4.4. Sample selection process .....	10-12
4.4.1. Inclusion criteria .....	11
4.4.2. Exclusion criteria .....	11
4.5. Image assessment and conditions .....	13

4.6. Data management .....	13
4.7. Statistical analysis .....	13-14
4.8. Ethical considerations .....	14
4.9. Budget .....	14
CHAPTER 5: RESULTS .....	15-28
5.1. Observations .....	15-19
5.2. Statistics .....	20-28
5.2.1. Overview .....	20
5.2.1.1. Contingency tables .....	21
5.2.1.2. Intra-observer agreement .....	22
5.2.1.3. Inter-observer agreement .....	23
5.2.1.4. Diagnostic tests .....	24
5.2.1.5. ROC curve analysis .....	25-27
5.2.1.6. Diagnostic odds ratio .....	28
5.2.1.7. McNemar's test .....	28
CHAPTER 6: DISCUSSION .....	29-34
6.1. Case examples .....	35-39
6.1.1. Case 1 .....	35
6.1.2. Case 2 .....	36
6.1.3. Case 3 .....	37
6.1.4. Case 4 .....	38
6.1.5. Case 5 .....	39
CHAPTER 7: CONCLUSION .....	40
CHAPTER 8: LIMITATIONS AND RECOMMENDATIONS .....	41-42
REFERENCES .....	43-51
APPENDICES .....	52-59
Appendix A: Eligible participants form.....	52
Appendix B: Radiographic assessment form.....	53
Appendix C: Letter requesting permission to view radiographic records.....	54
Appendix D: Authorization letter to access records.....	55
Appendix E: Ethics approval and project registration letter .....	56



Appendix F: STARD checklist ..... 57  
Appendix G: Formulae ..... 58-59



## LIST OF TABLES

<b>Table I.</b> Probable pathways for infections that originate in maxillary posterior teeth .....	8
<b>Table II.</b> Prevalence of maxillary apical lesion perforation .....	15
<b>Table III.</b> Study demographics .....	15
<b>Table IV.</b> Study population characteristics .....	16
<b>Table V.</b> Motive for CBCT referral .....	16
<b>Table VI.</b> Lesion site prevalence in the maxilla .....	17
<b>Table VII.</b> Lesion radiographic features .....	17
<b>Table VIII.</b> Associated tooth condition .....	18
<b>Table IX.</b> Lesion effect on tooth .....	18
<b>Table X.</b> Maxillary sinus mucosal lining changes .....	19
<b>Table XI.</b> Effect on mucosal lining .....	19
<b>Table XII.</b> 2 × 2 contingency table .....	21
<b>Table XIII.</b> CBCT contingency table .....	21
<b>Table XIV.</b> PAN contingency table .....	21



## LIST OF FIGURES

<b>Figure 1.</b> Flow diagram depicting throughput sequence of study population .....	12
<b>Figure 2.</b> CBCT Intra-observer agreement .....	22
<b>Figure 3.</b> PAN Intra-observer agreement .....	22
<b>Figure 4.</b> CBCT Inter-observer agreement .....	23
<b>Figure 5.</b> PAN Inter-observer agreement .....	23
<b>Figure 6.</b> Diagnostic test for CBCT .....	24
<b>Figure 7.</b> Diagnostic test for PAN .....	24
<b>Figure 8.</b> ROC curve analysis for CBCT .....	25
<b>Figure 9.</b> ROC curve graph for CBCT .....	25
<b>Figure 10.</b> ROC curve analysis for PAN .....	26
<b>Figure 11.</b> ROC curve graph for PAN .....	26
<b>Figure 12.</b> Comparative ROC curve analysis for CBCT vs. PAN .....	27
<b>Figure 13.</b> Comparative ROC curves graph for CBCT vs. PAN .....	27
<b>Figure 14.</b> DOR for CBCT vs PAN .....	28
<b>Figure 15.</b> McNemar's test for CBCT vs PAN .....	28
<b>Figure 16.</b> 6.1.1. Case 1 .....	35
<b>Figure 17.</b> 6.1.2. Case 2 .....	36
<b>Figure 18.</b> 6.1.3. Case 3 .....	37
<b>Figure 19.</b> 6.1.4. Case 4 .....	38
<b>Figure 20.</b> 6.1.5. Case 5 .....	39

## ACRONYMS AND ABBREVIATIONS

1D: One-dimensional  
2D: Two-dimensional  
3D: Three-dimensional  
AP: Apical periodontitis  
AUC: Area under the curve  
CBCT: Cone-beam computed tomography  
CI: Confidence interval  
CT: Computed tomography  
DOR: Diagnostic odds ratio  
FN: False negative  
FOV: Field of view  
FP: False positive  
FPD: Flat panel detector  
LR: Likelihood ratio  
MPR: Multi-planar reconstruction  
MRI: Magnetic resonance imaging  
*n*: Perforating apical lesions  
*N*: Sample size  
NPV: Negative predictive value  
OMS: Odontogenic maxillary sinusitis  
PAN: Pantomograph  
PPV: Positive predictive value  
RC: Radicular cyst  
RCT: Root canal treatment  
ROC: Receiver operating characteristic  
ROI: Region of interest  
STARD: Standards for reporting diagnostic accuracy  
TN: True negative  
TP: True positive



## GLOSSARY

**Diagnostic effectiveness (accuracy):** combined sensitivity and specificity into a single index of the probability of a positive result

**Diagnostic odds ratio (DOR):** the ratio of odds being positive in subjects with the disease to the odds being positive in subjects without disease

**False-negative (FN):** a test result indicating a subject doesn't have the disease when they essentially do

**False-positive (FP):** a test result indicating a subject has the disease when they essentially don't

**Likelihood ratio (LR):** probability ratio of the test result among subjects with the disease to those without

**McNemar's test:** a proportion analysis test for categorical outcome variables i.e. comparing matched-paired dichotomous outcome variables

**Negative predictive value (NPV):** the probability of not having the disease in a subject with a negative test result

**Positive predictive value (PPV):** the probability of having the disease in a subject with a positive test result

**Receiver operating characteristic (ROC):** a visual measure of intrinsic accuracy independent of disease prevalence presented graphically where the test's sensitivity is plotted on the  $y$ -axis versus its false-positive rate on the  $x$ -axis

**Sensitivity:** conditional probability of a positive test given that the subject has the disease

**Specificity:** conditional probability of a negative test given that the subject does not have the disease

**True negative (TN):** when a subject is without the disease and the test result correctly indicates so

**True positive (TP):** when a subject is with the disease and the test result correctly indicates so

**Youden's index ( $J$ ):** a single statistical outcome that captures the performance of dichotomous outcome variables by combining sensitivity and specificity



## CHAPTER 1: INTRODUCTION

The pantomograph (PAN) has been in use for decades in the field of dentistry and remains a vital diagnostic device. Popular as a screening tool, providing a generalized view of the maxillofacial region, it's not without limitations (Hallikainen, 1996). Rapid progression of advanced modalities such as cone-beam computed tomography (CBCT) has contributed vastly to the field of dentistry. CBCT has become more affordable with less exposure and exquisitely detailed images (Kiljunen *et al.*, 2015). Ongoing development ensures it's becoming refined and finding its way into daily practice. CBCT is not without drawbacks, as intricate images come with the responsibility to adequately interpret and report on all findings of the acquired volume (EADMFR, 2011).

Apical lesions can develop without an acute phase and no recollection of symptoms (Neville *et al.*, 2016). Often undergoing no significant radiographic or clinical change for a period of time (Cawson and Odell, 2008). Apical radiolucencies are found to be more apparent in molar teeth (Hussein *et al.*, 2016). With conventional radiography, especially in the maxilla, these frequently go undetected until significant bone loss has occurred, or the size and extensions are greatly underestimated (Lofthag-Hansen *et al.*, 2007; Venskutonis *et al.*, 2014).

High rates of infections in the maxillofacial region are of odontogenic origin. The complex anatomy of the head and neck area provides several pathways for infection spread (Rocha *et al.*, 2015). Maxillary posterior teeth approximation to the antrum risks these infections spreading via the sinus to other sites (Obayashi *et al.*, 2004). Subsequent complications can range from minor to fatal (Chapman *et al.*, 2013; Tataryn *et al.*, 2018).

The purpose of diagnostic accuracy studies is to assess by comparison the ability of diagnostic tests in identifying whether a target condition is present or absent. Biased and exaggerated results of diagnostic studies may result in the uptake of findings into clinical practice. The outcome can lead to an incorrect diagnosis, management, inappropriate testing, and increase in health-care cost. The skills to critically appraise the literature and adherence to clear standardised reporting of such studies are of importance (Anvari *et al.*, 2015; Cohen *et al.*, 2016; Durkan *et al.*, 2018; Obuchowski, 2005; Rutjes *et al.*, 2007; Schmidt and Factor, 2013).

## CHAPTER 2: LITERATURE REVIEW

### 2.1. Panoramic radiography

Radiographic examination of the dental patient is crucial for diagnosis, treatment planning and outcome evaluation (Rondon *et al.*, 2014). The dental pantomograph is a popular technique that provides a generalized view of the: maxilla, mandible and temporomandibular joints (Hallikainen, 1996). In the United Kingdom (UK) alone more than 2-million are taken per year, mostly by general dental practitioners (Murray and Whyte, 2002).

The principles of panoramic radiography follow conventional tomography (Hallikainen, 1996; Laney and Tolman, 1968). The cassette container or digital sensor and X-ray tube is at a fixed distance of 50-centimetres (cm) to 70 cm and rotate around the patients' head at the same time during exposure. With an effective dose ranging from 8.9-microsievert ( $\mu\text{Sv}$ ) to 37.8  $\mu\text{Sv}$  makes the practice of digital panoramic radiography relatively safe (Lee *et al.*, 2013). The holder or sensor moves in the same direction as the X-ray beam but at a slower speed. The correct speed ensures that the curved plane or image layer is in focus (Blackman, 1963). The image layer ranges between 10-millimetres (mm) to 30 mm thickness which includes the entire width of the jaw (Murray and Whyte, 2002).

The inherent limitations of two-dimensional (2D) panoramic radiography of three-dimensional (3D) anatomy are well known. These; include, unpredictable magnification, geometric distortion, low spatial resolution, and superimposition of anatomical structures that can hide important signs in the areas of interest (Devlin and Yuan, 2013; Dutra *et al.*, 2016; Kantor and Slome, 1989). Perceived to be a relatively simple imaging procedure to master, a study in the UK revealed that 33% of PANs produced were considered 'diagnostically unacceptable' (Murray and Whyte, 2002).

Even with its limitations, the PAN is considered an indispensable tool in patient screening, evaluation, and treatment. The availability, diagnostic value, low cost, low radiation exposure, and simplicity of the image acquisition compared to more advanced techniques; such as CBCT, conventional computed tomography (CT), and magnetic resonance imaging (MRI), makes the PAN invaluable in the dental practice (Rondon *et al.*, 2014).



## 2.2. Cone-beam computed tomography

Originally developed for angiography in the early '80s (Pauwels *et al.*, 2015). CBCT was conceptualized from hybridization between fluoroscopy and conventional CT. It is a relatively recent imaging modality with a wide range of applications; like orthodontics, maxillofacial, temporal, sino-nasal, radiotherapy planning, joint imaging, and the C-arm form used in interventional practice (Abramovitch and Rice, 2014). The naming of the imaging modality is due to the cone-shaped X-ray beam produced and projected onto a 2D flat panel detector (FPD) array. This arrangement is in contrast to conventional CT that produces a fan-shaped beam onto a one-dimensional (1D) arc-shaped curvilinear detector array (Boeddinghaus and Whyte, 2018).

The detector and X-ray beam rotate simultaneously 180° to 360° around the patient, who could be seated or standing while performing multi-base projections (Abrahamovitch and Rice, 2014). Complete imaging is obtained in a single rotation taking between 5-seconds (sec) and 30 sec (Venskutonis *et al.*, 2014). The multi-base projections raw volumetric data are reconstructed in 3D tomographic images and includes all anatomical planes. CBCT has a high spatial resolution due to the reconstructed data that consist of isotropic voxels (Kiljunen *et al.*, 2015). These voxels can be as small as 0.15 mm × 0.15 mm × 0.15 mm. The field of view (FOV) varies greatly amongst devices. There are four subcategories for FOV size which; include, dentoalveolar less than 8 cm, maxillomandibular between 8 cm to 15 cm, skeletal between 15 cm to 21 cm, and head and neck more than 21 cm (Venskutonis *et al.*, 2014).

Radiation dose is of concern regarding CBCT, being less than conventional CT but equal or more to the PAN. Low dose protocols can significantly reduce radiation dose; like smaller FOV, bigger voxel size, fewer projections, and pulsed compared to continuous beam acquisitions (Kiljunen *et al.*, 2015; Venskutonis *et al.*, 2014). In contrast, CBCT is an expensive, not readily available technique, where indiscriminate use can result in increased patient exposure (Lofthag-Hansen *et al.*, 2007; Noffke *et al.*, 2011).

CBCT has several advantages compared to other modalities. The 3D capabilities allow navigation in the: orthogonal-axial, -sagittal, -coronal, and non-orthogonal multi-planar reconstruction (MPR) views (Kiljunen *et al.*, 2015). This delivers precise unobstructed assessment of the anatomical

structures. The lack of distortion and magnification makes for accurate measurements (Kumar *et al.*, 2014; Lim *et al.*, 2018). These advantages are important in dental imaging which makes CBCT the preferred technique for complicated tooth impactions, implant planning, dental anomalies, selected dental inflammatory diseases, and dentoalveolar fractures (Boeddinghaus and Whyte, 2018; Hol *et al.*, 2015; Horner *et al.*, 2015). Disadvantages affecting image quality and diagnostic accuracy are the tendency for beam hardening and scatter caused by high-density materials and structures (Abrahamovitch and Rice, 2014; Matzen *et al.*, 2016). Inadequate calibration, patient movement, under-sampling, and volume averaging also negatively affect image quality (Lim *et al.*, 2018). It has very poor soft-tissue resolution and therefore alternate imaging techniques should be considered if such structures need evaluation. Conventional CT would be preferred for assessing, complicated dental infections, complex fractures, large odontogenic cysts or tumours, where information on soft tissue components may be of value. MRI with its high spatial- and superior soft tissue contrast-resolution is of use for staging oral malignancy, characterization of odontogenic lesions, and assessment of perineural tumour spread (Boeddinghaus and Whyte, 2018).

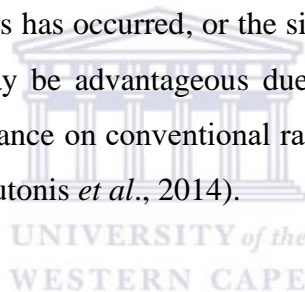
### **2.3. Periapical pathology**

Chronic apical periodontitis (AP) is a mass of subacute chronically inflamed granulation tissue at the apex of a non-vital tooth. Some chronic lesions develop without an acute phase and no recollection of previous symptoms. It results from a secondary defensive reaction in the presence of microbial infection in the tooth's root canal with subsequent spread of by-products into the apical area (Neville *et al.*, 2016). The predominant inflammatory cells present are neutrophils which release prostaglandins activating osteoclasts. As this reaction progress, osteoclastic apical bone resorption appears, when sufficient structure loss occurs, as a radiolucency at the tooth apex. Chronic lesions are usually asymptomatic and may undergo no significant radiographic or clinical change for a period of time (Cawson and Odell, 2008).

Distinguishing between chronic AP and a radicular cyst (RC) radiographically is in most cases not achievable and can only be done with histological analysis. A RC is defined as an epithelial lined periapical pouch of inflammatory origin. AP is osteolytic destruction due to inflammatory processes (Farman *et al.*, 1993). Definitive radiographic diagnosis has no effect on postoperative

implications therefore it's deemed an impractical exercise. These lesions are not necessarily inert and the inflammatory process can reactivate resulting in an enlargement. Reactivation is not always continuous and may occur sporadically (Neville *et al.*, 2016). Most are detected on routine dental radiographic examinations because of their asymptomatic tendency (Dutra *et al.*, 2016). Ranging from barely perceptible to very large on conventional radiographs. Due to the dynamic nature of inflammatory periapical lesions progression can be from chronic AP to an RC or an abscess by secondary infection and vice versa (Neville *et al.*, 2016).

The prevalence of apical radiolucencies is more apparent in molar teeth. Tooth related factors; such as inadequate root canal treatment (RCT), overfilling, underfilling, missed canals, post-placement, and defective coronal restorations are usual indicators. Patient age and gender have also been identified as related factors (Hussein *et al.*, 2016). Due to the nature of conventional radiography, especially in the maxilla with superimposing anatomical structures, most lesions go undetected until significant bone loss has occurred, or the size and extensions of a lesion may be greatly underestimated. CBCT may be advantageous due to the 3D capabilities in detecting periapical pathology prior to appearance on conventional radiography (Kamburoğlu *et al.*, 2017; Lofthag-Hansen *et al.*, 2007; Venskutonis *et al.*, 2014).



#### **2.4. The maxillary sinus**

The sinus cavity extends from the orbital floor to the alveolar segments of the maxilla and canine to the third molar area. As the ageing process continues so does the expansion of the maxillary sinus towards the tooth roots in the maxilla. This phenomenon is even more apparent in the edentulous (Cordero *et al.*, 2015). Expansion can lead to interdigitation of the sinus floor between adjacent teeth creating depressions and elevations with thin cortical areas. Radiographically tooth roots that appear to extend into the maxillary sinus do have a thin cortical layer of the bone surrounding the apical region (Roque-Torres *et al.*, 2015). In 14% to 28% of cases projection into the sinus may be apparent with a direct association between the tooth apices and the maxillary sinus mucosa (Lopes *et al.*, 2016). The apices of the 2<sup>nd</sup> molar have the closest association with the maxillary sinus followed by them; in descending order, 1<sup>st</sup> molar, 3<sup>rd</sup> molar, 2<sup>nd</sup> premolar, and 1<sup>st</sup> premolar (Cordero *et al.*, 2015).

There are several anatomic variations that can be associated with the sinus; like, antral septae, hypoplasia, or bony exostosis. Sinusitis, mucosal lining thickening, mucous retention cysts, polypoid lesions, foreign bodies, or discontinuation of the lateral wall are common findings. These variations are essential knowledge and the anatomy should be carefully examined when planning dental procedures in this area (Lozano-Carrascal *et al.*, 2017). Extractions, periodontal disease, implant treatment, or apical periodontitis increase the risk of pathological processes of odontogenic origin adjacent to the sinus (Roque-Torres *et al.*, 2015). Surgical violation of the sinus membrane is a regular occurrence and can cause odontogenic maxillary sinusitis (OMS). If left untreated OMS can progress to pansinusitis, and less commonly to meningitis, osteomyelitis or further intracranial spread of infection (Zirk *et al.*, 2017). Mild mucosal thickening is considered to be a normal radiographic finding, though, more than 2 mm of thickening may be related to an odontogenic pathological process (Bornstein *et al.*, 2012).

Conventional CT is considered to be the ‘gold standard’ in the visualization of the maxillary sinus, but CBCT has become increasingly popular in recent years (Constantine *et al.*, 2019). The shorter scanning time, decrease radiation dose, and higher resolution is advantageous when compared to CT (Shanbhag *et al.*, 2013). The 3D imaging capabilities of CBCT improves visualization and early diagnosis of suspected odontogenic and sinus related pathologies in the maxilla (Santos *et al.*, 2015). It has been shown that detection of apical pathologies in maxillary molars and premolars may be mis- or undiagnosed with conventional radiographs. Compared to CBCT where pathology was successfully identified (Bornstein *et al.*, 2012).

## **2.5. Spread of odontogenic infections in the maxillary teeth**

Maxillofacial infections of odontogenic origin contribute to a high percentage of the overall infections in this area. The complex anatomy of this region consists of numerous compartments formed by fascia and muscles providing pathways for spread. There are various infection pathways from the maxillary teeth (Rocha *et al.*, 2015). Upper regions can include the maxillary sinus from posterior teeth. Subsequent soft tissue involvement is multifaceted due to intricate anatomical structures (Obayashi *et al.*, 2004).

Complications from such can range from minor to severe or even fatal. Subperiosteal and extraosseous abscess formation can: penetrate bone, cause fistulisation, and spread into adjacent soft tissue. Followed by soft-tissue swelling, oedema, and fluid collection (Chapman *et al.*, 2013). Sinusitis of odontogenic origin is well documented and is thought to be accountable for 10% to 12% of all cases. The infection spreads from the apical foramina of a tooth disrupting the Schneiderian membrane and creating a path to the maxillary sinus (Tataryn *et al.*, 2018).

Fascial space infections can occur from chronic lesions and inflammation. When deep neck regions are affected morbidity and mortality rates increase drastically. Inferior progression can involve the mediastinum with subsequent mediastinitis (Rocha *et al.*, 2015). A rare complication includes orbital inflammation where prompt treatment is required, as irreversible damage to vision can result. Pathways leading to orbital inflammation; include, direct extension from maxillary sinus disease, infection via the premaxillary soft tissues, and spread from the posterior maxillary teeth via the masticator space into the infratemporal fossa and inferior orbital fissure. Intracranial complications, although rare, can be fatal. Septic thrombosis of the venous sinuses occurs from facial infections including sinus disease and orbital cellulitis which may have originated from an apical or periodontal infection. Osteomyelitis can result from inadequate initial treatment, chronic infections, or in immunocompromised patients (Chapman *et al.*, 2013).

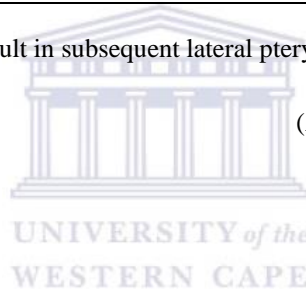
It has been suggested that involvement of the maxillary sinus can occur via all maxillary posterior teeth. Succeeding fascial space spread vary depending on the tooth origin (Table 1). Infection pathways in the maxillary region are determined by multiple factors; including, site origin, tooth positioning, fascial spaces, and underlying muscles (Drake *et al.*, 2014; Obayashi *et al.*, 2004).

**Table I.** Probable pathways for infections that originate in maxillary posterior teeth

<b>Origin</b>	<b>Fascial space</b>	<b>Muscle</b>
<b>1<sup>st</sup> Premolar</b>	Buccal	Levator anguli oris; Buccinator
<b>2<sup>nd</sup> Premolar</b>	Buccal	Buccinator
<b>1<sup>st</sup> Molar</b>	Buccal	Buccinator
<b>2<sup>nd</sup> Molar</b>	Buccal; Masticator†	Buccinator; Masseter; Temporal
<b>3<sup>rd</sup> Molar</b>	Masticator†; Parapharyngeal	Medial pterygoid

† Masticator space involvement result in subsequent lateral pterygoid involvement

(Adapted from Obayashi *et al.*, 2004)



## **2.6. Inference**

Existing literature shows that apical pathology in posterior teeth of the maxilla is a common and well-documented occurrence. Although to date no comparative study of imaging modalities evaluating apical pathology ‘perforating’ or ‘breaching’ the cortical plate into the maxillary sinus was found. Nor documentation of prevalence and incidence. Therefore, this comparative study may give some insight into this phenomenon.

## CHAPTER 3: AIM AND OBJECTIVES

### 3.1. Aim

To evaluate the diagnostic accuracy of PAN and CBCT images related to maxillary posterior teeth periapical pathology that perforates the floor of the maxillary sinus by comparing the two radiographic modalities.

### 3.2. Objectives

- To assess periapical pathology perforating the maxillary sinus in CBCT images
- To assess periapical pathology perforating the maxillary sinus in PAN images
- To compare the diagnostic accuracy of PAN to CBCT images



## CHAPTER 4: MATERIALS AND METHODS

### 4.1. Study design

This was a retrospective cross-sectional diagnostic accuracy study (i.e. ‘classical’ diagnostic accuracy study design).

### 4.2. Equipment

CBCT acquisitions were from a NewTom® VGi with NNT® software (version 8). The CBCT volume evaluation was performed on a Barco® Eonis© 22-inch MDRC-2122, resolution 1920 × 1080 monitor and Personal computer (PC) tower Hewlett-Packard®, HP® Z240 Tower workstation comprising of an Intel® Xeon® CPU E3-1270 v5 @ 3.60GHz, 8.00 GB RAM, 64-bit Operating System, x64-based processor, running Windows® 10 Enterprise, Version 1709, © 2017 Microsoft Corporation, AMD Incorporation, Radeon® RX 550 series.

PAN acquisitions were from a Sirona® Orthophos® XG 3 and 5 with Sidexis® software (version 4). The PAN image evaluation was performed on a Barco® Eonis© 22-inch MDRC-2122, resolution 1920 × 1080 monitor and Dell® G5 15 laptop comprising of an Intel Core i7-8750H CPU @ 2.20GHz, 16 GB RAM, 64-bit Operating System, x64-based processor, running Windows® 10 Pro, © 2019 Microsoft Corporation, NVIDIA Corporation, GeForce® GTX 1050 Ti.

### 4.3. Target population

The study population was selected manually comprising of patient records from the Department of Diagnostics and Radiology, Faculty of Dentistry, University of the Western Cape, Tygerberg, Cape Town, South Africa spanning the period of January 2016 to December 2019.

### 4.4. Sample selection process

All CBCT volumes in the designated time period were evaluated for patients with apical lesions in the maxilla i.e. consecutive sampling. Potentially eligible participants qualifying according to the inclusion and exclusion criteria in line with the aim and objectives of the study were selected. The corresponding PANs were obtained adhering to the selection criteria resulting in eligible



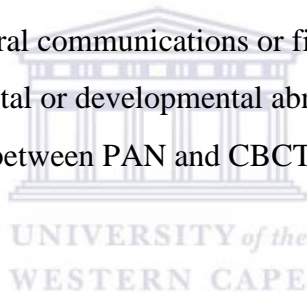
participants. Recording of patient records was done on the 'Eligible participants form' (Appendix A) by the main researcher. Patient radiographic images were exported as DICOM files and deidentified with DicomCleaner™ PixelMed Publishing™.

#### **4.4.1. Inclusion criteria**

- Maxillary teeth (14,15,16,17,18,24,25,26,27,28)
- Patients with already performed and available PAN and CBCT image records
- High-resolution radiographic images of adequate diagnostic quality
- Patient ages between 18 and 80 years

#### **4.4.2. Exclusion criteria**

- Dental implants in the region of interest (ROI)
- Trauma in the ROI
- Patients with oral antral communications or fistulas (OAC, OAF) in the ROI
- Patients with congenital or developmental abnormalities in the ROI
- Acquisition interval between PAN and CBCT more than 6 months



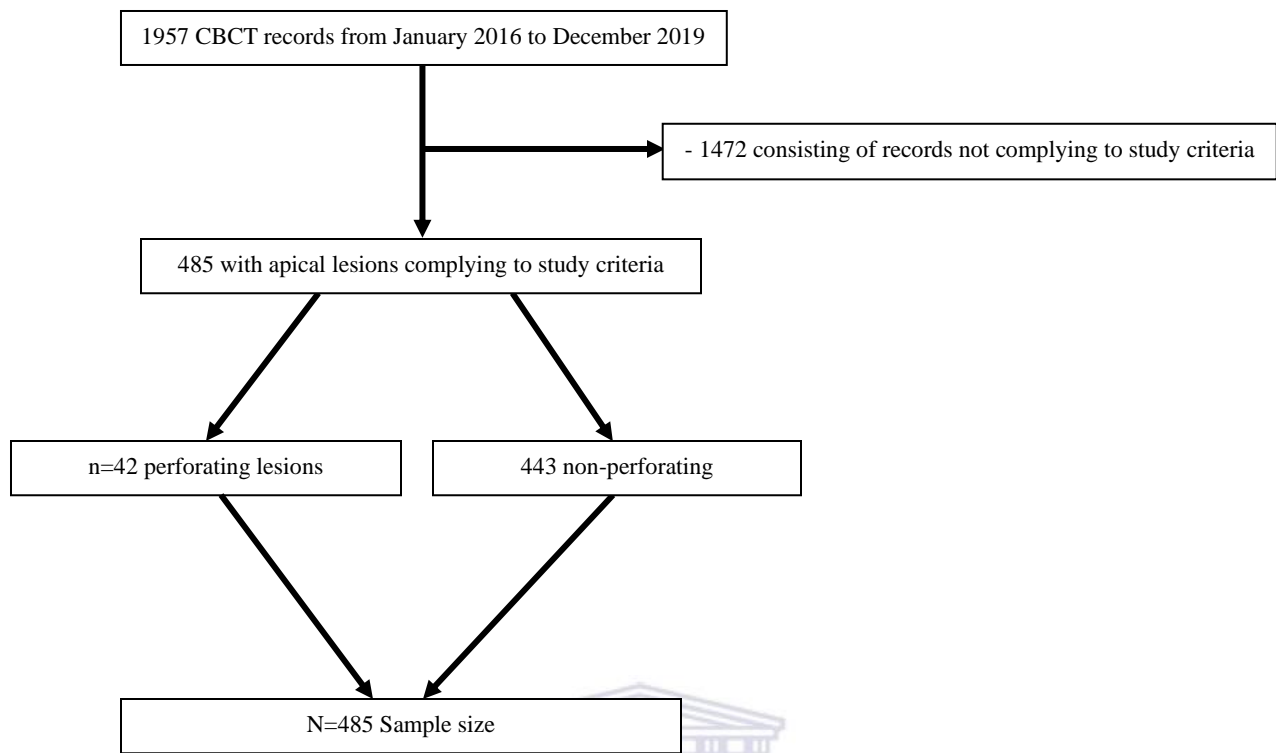


**Figure 1.** Flow diagram depicting throughput sequence of study population.



#### **4.5. Image assessment and conditions**

Systematic randomizing techniques consisting of a container with the anonymized subjects and blinded raffle picking were employed prior to presenting the patient acquisitions for radiographic evaluation. Radiographic evaluation of images was recorded according to the ‘Radiographic assessment form’ (Appendix B). During radiographic assessment viewing of PAN images and CBCT volumes was done under ambient lighting. Image/volume navigation and manipulation with regards to magnification, brightness, contrast, creating volume renders and custom-sections was allowed. No clinical information was provided and no time limit was imposed during the assessment. Perforation of the maxillary sinus floor by apical pathology was defined as the presence of apical pathology with subsequent clear interruption/discontinuation of the cortex at the region of interest. Perforation on CBCT volumes was visualized in at least 1 mm slice thickness and confirmed in two planes. The primary observer was presented with the total sample ( $N$ ) for radiographic evaluation. Subsequent evaluation of  $\approx 10$  per cent of  $N$  was performed by the primary observer as well a secondary, senior member of the department, for intra- and inter-observer agreement.

#### **4.6. Data management**

The raw data were recorded in Microsoft Office Excel® 2016 (Microsoft Corp., Redmond, WA) spreadsheet and imported for statistical analysis to MedCalc® Statistical Software version 19.1.5 (MedCalc Software bv, Ostend, Belgium; <https://www.medcalc.org>; 2020).

The data was periodically stored on 2 secure, password-protected sources namely a laptop, HP® Intel® Core™ i3-5005U CPU @ 2.00 GHz, 4.00GB RAM, 64-bit Operating System, x64-based processor, running Windows® 10 Pro, © 2018 Microsoft Corporation and a portable external hard drive, Transcend® StoreJet® 25H3, 1TB.

#### **4.7. Statistical analysis**

Statistical analysis was performed ‘only’ on the categorical dichotomous variable of maxillary periapical pathology perforating the sinus floor i.e. presence or absence thereof on both modalities. The CBCT is the reference standard. Remaining data were solely reported on. Cohen’s kappa ( $\kappa$ ) statistic was applied to assess observer agreement. Values of sensitivity, specificity, positive

predictive value (PPV), negative predictive value (NPV), diagnostic effectiveness (i.e. accuracy), Diagnostic Odds Ratio (DOR) and Likelihood Ratio (LR) was calculated. Receiver Operating Characteristic (ROC) curves were plotted with the calculation of the Area Under the Curve (AUC). A succeeding comparison among PAN and CBCT findings was done using the McNemar's test. The null hypothesis ( $H_0$ ) was set that the two diagnostic tests capabilities in detecting the investigated entity are equal. The alternate hypothesis ( $H_1$ ) was set that the two tests capabilities in detecting the investigated entity are not equal. Calculations were done with a 95% confidence interval (CI) and P-values less than 0.05 was considered to be statistically significant unless stated otherwise.

#### **4.8. Ethical considerations**

This was a retrospective study and no radiographic acquisitions were performed for the sole purpose of this study. All radiographic acquisitions were performed by experienced and trained personnel under routine daily conditions. Patient confidentiality was maintained by allocating numbers to the records and data files was deidentified by use of speciality software. Use of patient records was officially requested (Appendix C) and approved by the principal administrator of the establishment (Appendix D). This study was proposed to the designated faculty and subsequent ethics approval and project registration were obtained (Appendix E).

#### **4.9. Budget**

This research was a self-funded project.

## CHAPTER 5: RESULTS

### 5.1. Observations

The total of CBCT volumes from January 2016 to December 2019 analysed was 1957. Cases selected based on the study's parameters included  $N=485$  of participants with apical lesions. Of  $N$ , the total for perforated lesions consisted of  $n=42$  and non-perforated lesions 443, with a ratio of 1:11. Calculation of perforation prevalence amongst apical lesions  $(n \div N) \times 100 = x$  expressed as a percentage result in 8.66% (Table II).

**Table II.** Prevalence of maxillary apical lesion perforation

Sample size ( $N$ )	Perforated ( $n$ )	Non-perforated	Ratio	Prevalence
485	42	443	1:11	8.6597≈8.66%

Of the 42 cases, the largest percentile 35.7% placed in the 18 to 30 years age group; with the second largest of 19% amongst the 31 to 40 years and 51 to 60 respectively; thirdly age group 41 to 50 consisted of 16.7%, and finally both age groups 61 to 70 and 71 to 80 comprised of 4.8% respectively (Table III).

**Table III.** Study demographics

Age group	No. records	Frequency	No. females	No. males
18-30	15	35.7%	7	8
31-40	8	19.0%	2	6
41-50	7	16.7%	3	4
51-60	8	19.0%	5	3
61-70	2	4.8%	0	2
71-80	2	4.8%	1	1
<b>Total</b>	<b>42</b>	<b>100</b>	<b>18</b>	<b>24</b>

†Age in years

The maximum age was 71 years consisting of two cases; the minimum was one case of 18 years old. The average age of occurrence was 40 years with a median of 37.5 years. Gender distribution amongst cases included 28 males and 18 females. With a male to female ratio of 1.3:1 (Table IV).

**Table IV.** Study population characteristics

<b>Maximum age</b>	71
<b>Minimum age</b>	18
<b>Average age</b>	40
<b>Median age</b>	37.5
<b>Gender ratio</b>	1.3 Male:1 Female

†Age in years

Based on the referral motive (main complaint) for CBCT acquisitions the majority, 31 %, consisted of restorative purposes especially implant treatment (single or multiple units) and prosthodontic full-mouth rehabilitation. Following 26% for trauma and unrelated pathology respectively. 5% of cases included orthodontic planning of which one case was for pre-orthognathic surgery. 12% of the referrals were related to the ROI and related studied pathology (Table V).

**Table V.** Motive for CBCT referral

<b>Main complaint</b>	<b>No. records</b>	<b>Frequency</b>
<b>ROI (i.e. apical pathology)</b>	5	12%
<b>Trauma</b>	11	26%
<b>Unrelated pathology (i.e. infection, cysts, neoplasms)</b>	11	26%
<b>Restorative (i.e. implants)</b>	13	31%
<b>Orthodontics (incl. orthognathics)</b>	2	5%
<b>Total</b>	<b>42</b>	<b>100%</b>

The first molar was the most common site of occurrence consisting of 47.5% of cases. The most commonly affected tooth was the 26 consisting of 12 cases. Least likely was the 15 and 24 each with one case respectively. When comparing the quadrants in the maxilla the 1<sup>st</sup> quadrant entailed 18 cases with the 2<sup>nd</sup> quadrant 24 giving an incidence ratio of 1:1.3 (Table VI).

**Table VI.** Lesion site prevalence in the maxilla

Affected tooth	1 <sup>st</sup> Quadrant	2 <sup>nd</sup> Quadrant	Frequency
1 <sup>st</sup> Premolar	2	1	7.0%
2 <sup>nd</sup> Premolar	1	3	10.0%
1 <sup>st</sup> Molar	8	12	47.5%
2 <sup>nd</sup> Molar	5	6	26.0%
3 <sup>rd</sup> Molar	2	2	9.5%
<b>Total</b>	<b>18</b>	<b>24</b>	<b>100%</b>

Lesion size was measured in millimetres on the respective modalities and their manufacturer supplied accompanying software. PAN measurements were done as the maximum dimensions in two planes with a resulting average amongst *n* as 5.4 mm × 5.6 mm. CBCT measurements were done as the maximum dimensions in three planes with a resulting average amongst *n* as 4.9 mm × 4.8 mm × 5.6 mm. The internal radiographic appearance in 100% of cases appeared as radiolucent on PANs and as a low-density on CBCTs respectively. Both modalities demonstrated the majority of lesions as well-defined: 72% on PAN images and 67% on CBCT slices (Table VII).

**Table VII.** Lesion radiographic features

	PAN	CBCT
<b>Smallest</b> †	1.4 × 2.4	2.7 × 1.2 × 2.4
<b>Largest</b> †	17.9 × 16.3	10.3 × 13 × 14.2
<b>Average</b> †	5.4 × 5.6	4.9 × 4.8 × 5.6
<b>Lucent/low-density</b>	100%	100%
<b>Well-defined</b>	72%	67%
<b>Ill-defined</b>	28%	33%

† Measurements are in millimetres (mm)

The majority of cases, 40.4%, was associated with an only carious tooth. Followed by 28.6% endodontically treated; 23.8% restored teeth; 4.8% seemingly sound; and one surgically treated tooth (Table VIII). The studied pathology as per CBCT evaluation had no subsequent effect on tooth position in the majority of cases, 88%, where's 12% appeared to be elevated (Table IX).

**Table VIII.** Associated tooth condition

	<b>No. records</b>	<b>Frequency</b>
<b>Sound</b>	2	4.8%
<b>Carious</b>	17	40.4%
<b>Restored</b>	10	23.8%
<b>Endodontically treated</b>	12	28.6%
<b>Surgically treated</b>	1	2.4%
<b>Total</b>	<b>42</b>	<b>100%</b>

**Table IX.** Lesion effect on tooth

	<b>No. records</b>	<b>Frequency</b>
<b>Tooth elevated</b>	5	12%
<b>No effect</b>	37	88%
<b>Total</b>	<b>42</b>	<b>100%</b>

†Results according to CBCT



40 of the 42 cases as per CBCT evaluation, which translates to 95% of *n* presented with some form of maxillary sinus mucosal lining reaction (Table X). 77.5% of these presented with mucositis; 12.5% with a mucocele; and the remaining 10% with a polyp/mucous retention pseudocyst (Table XI). CBCT evaluation revealed seven cases with a marked fluid level in the associated maxillary sinus antrum.

**Table X.** Maxillary sinus mucosal lining changes

	<b>No. records</b>	<b>Frequency</b>
<b>Present</b>	40	95%
<b>Absent</b>	2	5%
<b>Total</b>	<b>42</b>	<b>100%</b>

†Results according to CBCT

**Table XI.** Effect on mucosal lining

	<b>No. records</b>	<b>Frequency</b>
<b>Mucositis</b>	31	77.5%
<b>Polyp/mucous retention pseudo cyst</b>	4	10%
<b>Mucocele</b>	5	12.5%
<b>Total</b>	<b>40†</b>	<b>100%</b>

†Total presenting mucosal changes

‡Results according to CBCT

## 5.2. Statistics

### 5.2.1. Overview

Cohen's kappa ( $\kappa$ ) statistic was applied for observer agreement. The intra-observer agreement obtained was 0.80128 for CBCT (Figure 2) and 0.78947 for PAN (Figure 3). The inter-observer agreement obtained was 0.73333 for CBCT (Figure 4) and 0.64444 for PAN (Figure 5).

Calculated disease prevalence of 8.66% was used for diagnostic tests. CBCT as the 'reference standard' showed: 100% sensitivity, specificity, PPV, NPV, and accuracy (Figure 6). ROC curve analysis indicated Youden's index at 1.000, an AUC of 1.000, LR+ to  $\infty$ , and LR- of 0.00 (Figure 8).

PAN diagnostic tests yielded: 14.286% sensitivity, 79.910% specificity, 6.316% PPV, 90.769% NPV, and 74.227% accuracy (Figure 7). ROC curve analysis showed Youden's index at 0.05805, an AUC of 0.529, LR+ of 1.07, and LR- of 0.71 (Figure 10).

Comparative tests of the modalities; included, a comparison ROC curve analysis which showed difference in AUC of 0.471, z-statistic result of 10.447, significance level of  $P < 0.0001$  (Figure 12), DOR calculation with 0.6629 (Figure 14), and McNemar's test revealed a significance level of  $P < 0.0001$  (Figure 15).

### 5.2.1.1. Contingency tables

**Table XII.**  $2 \times 2$  contingency table

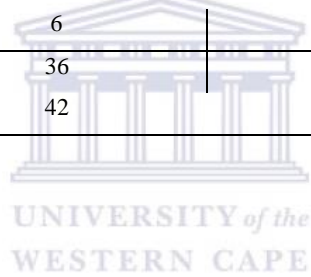
	Disease PRESENT+	Disease ABSENT-	Total
Test POS+	<b>TP</b>	<b>FP</b>	
Test NEG-	<b>FN</b>	<b>TN</b>	
<b>Total</b>			

**Table XIII.** CBCT contingency table

	Disease PRESENT+	Disease ABSENT-	Total
Test POS+	42	0	42
Test NEG-	0	443	443
<b>Total</b>	42	443	<b>485</b>

**Table XIV.** PAN contingency table

	Disease PRESENT+	Disease ABSENT-	Total
Test POS+	6	89	42
Test NEG-	36	354	443
<b>Total</b>	42	443	<b>485</b>



### 5.2.1.2. Intra-observer agreement

Observer A	Observer_1_Round_1_CBCT		
Observer B	Observer_1_Round_2_CBCT		
	Observer_1_Round_1_CBCT		
Observer_1_Round_2_CBCT	0	1	
0	41	2	43 (89.6%)
1	0	5	5 (10.4%)
	41 (85.4%)	7 (14.6%)	48
Kappa	0.81028		
Standard error	0.12894		
95% CI	0.55754 to 1.00000		

**Figure 2.** CBCT Intra-observer agreement.

Observer A	Observer_1_Round_1_PAN		
Observer B	Observer_1_Round_2_PAN		
	Observer_1_Round_1_PAN		
Observer_1_Round_2_PAN	0	1	
0	45	1	46 (95.8%)
1	0	2	2 (4.2%)
	45 (93.7%)	3 (6.2%)	48
Kappa	0.78947		
Standard error	0.20365		
95% CI	0.39031 to 1.00000		

**Figure 3.** PAN Intra-observer agreement.

### 5.2.1.3. Inter-observer agreement

Observer A	Observer_1_CBCT		
Observer B	Observer_2_CBCT		
	Observer_1_CBCT		
Observer_2_CBCT	0	1	
0	40	2	42 (87.5%)
1	1	5	6 (12.5%)
	41 (85.4%)	7 (14.6%)	48
Kappa	0.73333		
Standard error	0.14578		
95% CI	0.44761 to 1.00000		

**Figure 4.** CBCT Inter-observer agreement.

Observer A	Observer_1_PAN		
Observer B	Observer_2_PAN		
	Observer_1_PAN		
Observer_2_PAN	0	1	
0	44	1	45 (93.7%)
1	1	2	3 (6.2%)
	45 (93.7%)	3 (6.2%)	48
Kappa	0.64444		
Standard error	0.23336		
95% CI	0.18705 to 1.00000		

**Figure 5.** PAN Inter-observer agreement.

### 5.2.1.4. Diagnostic tests

#### Data

	Disease Present	Disease Absent	
	42	0	42
	0	443	443
	42	443	

#### Results

Sensitivity	100.000%	91.592% to 100.000%
Specificity	100.000%	99.171% to 100.000%
AUC	1.000	0.992 to 1.000
Positive Likelihood Ratio		
Negative Likelihood Ratio	0.000	
Disease prevalence	8.660%	
Positive Predictive Value	100.000%	
Negative Predictive Value	100.000%	
Accuracy	100.000%	99.242% to 100.000%

**Figure 6.** Diagnostic test for CBCT.



#### Data

	Disease Present	Disease Absent	
	6	89	95
	36	354	390
	42	443	

#### Results

Sensitivity	14.286%	5.428% to 28.539%
Specificity	79.910%	75.871% to 83.543%
AUC	0.471	0.426 to 0.516
Positive Likelihood Ratio	0.711	0.331 to 1.526
Negative Likelihood Ratio	1.073	0.940 to 1.224
Disease prevalence	8.660%	
Positive Predictive Value	6.316%	3.045% to 12.641%
Negative Predictive Value	90.769%	89.602% to 91.817%
Accuracy	74.227%	70.091% to 78.065%

**Figure 7.** Diagnostic test for PAN.

### 5.2.1.5. ROC curve analysis

Variable	CBCT											
Classification variable	CBCT											
Sample size	485											
Positive group <sup>a</sup>	42 (8.66%)											
Negative group <sup>b</sup>	443 (91.34%)											
<sup>a</sup> CBCT = 1												
<sup>b</sup> CBCT = 0												
Disease prevalence (%)	8.66											
<b>Area under the ROC curve (AUC)</b>												
Area under the ROC curve (AUC)	1.000											
Standard Error <sup>a</sup>	0.000											
95% Confidence interval <sup>b</sup>	0.992 to 1.000											
Significance level P (Area=0.5)	<0.0001											
<sup>a</sup> Hanley & McNeil, 1982												
<sup>b</sup> Binomial exact												
<b>Youden index</b>												
Youden index J	1.0000											
Associated criterion	>0											
Sensitivity	100.00											
Specificity	100.00											
<b>Criterion values and coordinates of the ROC curve [Hide]</b>												
Criterion	Sensitivity	95% CI	Specificity	95% CI	+LR	95% CI	-LR	95% CI	+PV	95% CI	-PV	95% CI
≥0	100.00	91.6 - 100.0	0.00	0.0 - 0.8	1.00	1.0 - 1.0			8.7	8.7 - 8.7		
>0	100.00	91.6 - 100.0	100.00	99.2 - 100.0			0.00		100.0		100.0	
>1	0.00	0.0 - 8.4	100.00	99.2 - 100.0			1.00	1.0 - 1.0			91.3	91.3 - 91.3

Figure 8. ROC curve analysis for CBCT.

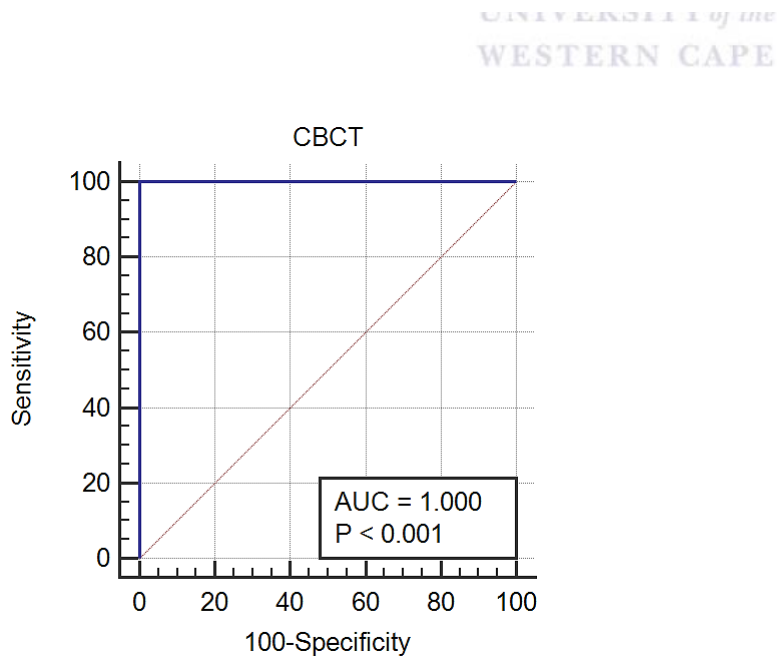


Figure 9. ROC curve graph for CBCT.

Variable	PAN
Classification variable	CBCT
Sample size	485
Positive group <sup>a</sup>	42 (8.66%)
Negative group <sup>b</sup>	443 (91.34%)

<sup>a</sup> CBCT = 1

<sup>b</sup> CBCT = 0

Disease prevalence (%)	8.66
------------------------	------

**Area under the ROC curve (AUC)**

Area under the ROC curve (AUC)	0.529
Standard Error <sup>a</sup>	0.0451
95% Confidence interval <sup>b</sup>	0.484 to 0.574
z statistic	0.644
Significance level P (Area=0.5)	0.5197

<sup>a</sup> Hanley & McNeil, 1982

<sup>b</sup> Binomial exact

**Youden index**

Youden index J	0.05805
Associated criterion	≤0
Sensitivity	85.71
Specificity	20.09

**Criterion values and coordinates of the ROC curve [Hide]**

Criterion	Sensitivity	95% CI	Specificity	95% CI	+LR	95% CI	-LR	95% CI	+PV	95% CI	-PV	95% CI
<0	0.00	0.0 - 8.4	100.00	98.2 - 100.0	1.00	1.0 - 1.0	1.00	1.0 - 1.0				
≤0	85.71	71.5 - 94.6	20.09	16.5 - 24.1	1.07	0.9 - 1.2	0.71	0.3 - 1.5	9.2	8.2 - 10.4	93.7	87.4 - 97.0
≤1	100.00	91.6 - 100.0	0.00	0.0 - 0.8	1.00	1.0 - 1.0			8.7	8.7 - 8.7		

||| ||| ||| ||| ||| |||

**Figure 10.** ROC curve analysis for PAN.

UNIVERSITY of the  
WESTERN CAPE

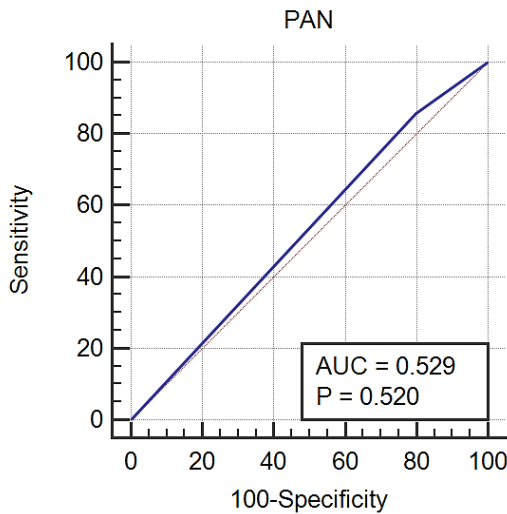


**Figure 11.** ROC curve graph for PAN.



Variable 1	CBCT
Variable 2	PAN
Classification variable	CBCT

Sample size	485
Positive group <sup>a</sup>	42 (8.66%)
Negative group <sup>b</sup>	443 (91.34%)

<sup>a</sup> CBCT = 1

<sup>b</sup> CBCT = 0

Variable	AUC	SE <sup>a</sup>	95% CI <sup>b</sup>
CBCT	1.000	0.000	0.992 to 1.000
PAN	0.529	0.0451	0.484 to 0.574

<sup>a</sup> Hanley & McNeil, 1982

<sup>b</sup> Binomial exact

#### Pairwise comparison of ROC curves

CBCT ~ PAN	
Difference between areas	0.471
Standard Error <sup>a</sup>	0.0451
95% Confidence Interval	0.383 to 0.559
z statistic	10.447
Significance level	P < 0.0001

<sup>a</sup> Hanley & McNeil, 1983

**Figure 12.** Comparative ROC curve analysis for CBCT vs. PAN.

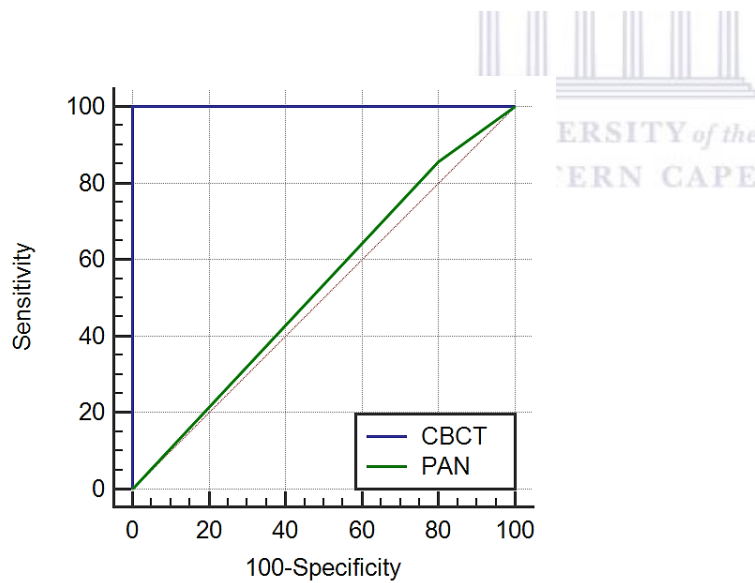


**Figure 13.** Comparative ROC curves graph for CBCT vs. PAN.

### 5.2.1.6. Diagnostic odds ratio

Outcome	PAN		
Group	CBCT		
	CBCT		
PAN	0	1	
0	354	36	390 (80.4%)
1	89	6	95 (19.6%)
	443	42	485
Odds ratio	0.6629		
95% CI	0.2709 to 1.6224		
z statistic	0.900		
Significance level	P = 0.3680		

Figure 14. DOR for CBCT vs PAN.

### 5.2.1.7. McNemar's test

Classification A	CBCT		
Classification B	PAN		
	PAN		
CBCT	0	1	
0	354	89	443 (91.3%)
1	36	6	42 (8.7%)
	390 (80.4%)	95 (19.6%)	485

#### McNemar test

Difference	10.93%
95% CI	6.52 to 15.34

#### Exact probability (binomial distribution)

Significance	P < 0.0001
--------------	------------

Figure 15. McNemar's test for CBCT vs PAN.

## CHAPTER 6: DISCUSSION

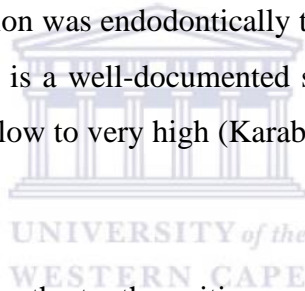
Although numerous studies regarding apical lesions and AP can be found in the literature. To current knowledge, none were found related specifically to lesions perforating the maxillary sinus floor. Thus, for reference, the results in this study were relatively compared to literature pertaining to non-specific AP and apical lesions.

A review in 2017 regarding AP epidemiology concluded on a patient level, i.e. one or more lesion per patient, the prevalence ranged from 7% to 86% with a median of 52.5%. Primary AP was from 10% to 53% with a median of 20.3% and RCT'd teeth from 20% to 82% with a median of 61%. Prevalence with regards to tooth level was 2% to 14% with a median of 6%. A previous review in 2009 concluded primary AP to range from 1% to 13% with a median of 3.5%. RCT'd teeth ranged from 2% to 18% and a median of 6% (Karabucak *et al.*, 2016; Persoon and Özok, 2017; Van der Veken *et al.*, 2017). AP prevalence studies can be greatly affected by several factors such as systemic (e.g. diabetes), social (e.g. smoking), and region where access to oral healthcare may be limited as in developing countries.

In consideration of AP prevalence in other parts of the world even with excluded records in this study the remaining 485 with apical lesions out of 1957 records remains a relatively high percentage (Table II). This extrapolation may be explained due to geographical location. Studies based on the decayed, missing and filled teeth (DMFT) index scoring has shown that the Western Cape Province has the highest dental caries rate amongst children in South Africa. The prevalence amongst ages 4 to 15 years has steadily increased from 2002 to 2015. In the Western Cape, about 80% of carious lesions remain untreated in children age 6 years. The South African average is 45% to 60% and a mean number of teeth needing treatment are 2 to 3 (Mohamed and Barnes, 2018; Singh, 2011; Smit *et al.*, 2017).

The calculated prevalence of apical lesions perforating compared to non-perforated in the current study's population was 8.66% with a ratio of 1:11 (Table II). In consideration of the high caries rate in the province, perforating lesion prevalence, and CBCT referral motive (main complaint) only 12% was related to the ROI (Table V). This correlates to the well-known fact that these

lesions may go undetected because of asymptomatic tendencies (Cawson and Odell, 2008; Dutra *et al.*, 2016). The vast majority of referrals consist of advanced restorative treatment, trauma, and unrelated pathology. Lacking clinical expertise whereby clinicians fail to recognize lesions or are reluctant to investigate further may contribute to this finding. The median age was 37.5 years, average age 40 years with a slight male predominance in a ratio of 1.3:1. The gender distribution difference appears negligible. The mean and average age is situated at the border of the 4<sup>th</sup> and 5<sup>th</sup> decade (Table IV). Associative factors can relate to disease prevalence, higher likelihood of extensive dental work, age-related comorbidities, and a low life expectancy in South Africa averaging at the lower limits of the 7<sup>th</sup> decade (Jaul and Barron, 2017; Mckenna, and Burke, 2010). Associated tooth condition was predominated by 40.4% primarily carious teeth (Table VIII). South Africa a developing country with a large population of low-socioeconomic status individuals, limited access to adequate oral healthcare, and high caries rate in the Western Cape correlates to this finding (Mohamed and Barnes, 2018; Singh, 2011; Smit *et al.*, 2017). The second largest group related to tooth condition was endodontically treated teeth consisting of 28.6% of *n* (Table VIII). The RCT failure rate is a well-documented subject with AP prevalence amongst treated teeth reported to range from low to very high (Karabucak *et al.*, 2016; Persoon and Özok, 2017; Van der Veken *et al.*, 2017).



Only 12% of lesions had an effect on the tooth position, resulting in tooth elevation (Table IX). This may be due to disease pathogenesis and anatomical variations. The maxillary antrum being an empty cavity of air where resulting perforation can lead to decompression and failure in confinement of the lesion. Approximation of the roots to the antrum with the disease process following the path of least resistance may contribute. Obayashi *et al* (2004) demonstrated that odontogenic apical lesions and related pathways of infection in the maxilla are more likely to perforate buccally compared to the palate and maxillary floor. The main contributing factor being a thinner buccal cortical plate.

CT based prevalence studies of the maxillary sinus revealed more than half of the general population have some sinus-related abnormality (Drumond *et al.*, 2017; Guerra-Pereira *et al.*, 2015). A study revealed that the PAN has very low efficacy in diagnosing sinus disease when compared to CBCT (Constantine *et al.*, 2019). More than half of known maxillary sinusitis cases

on CBCT images was shown to be of odontogenic origin. Up to 86% of routine dental examinations that included conventional radiographs failed to recognize OMS. The current study demonstrated mucosal lining changes in up to 95% of *n* based on CBCT findings (Table X). This coincides with previous studies where up to 100% of all AP lesions demonstrated mucosal lining changes. The first maxillary molar was the most commonly affected tooth by a vast majority in the 1<sup>st</sup> and 2<sup>nd</sup> quadrant (Table VI). Previous studies on odontogenic apical lesions/infections demonstrated similar findings. Caries prevalence rates and the tooth being first to erupt at the age of 6 years persisting in situ for the remainder of life correlates to the high likelihood (Obayashi *et al.*, 2004; Tataryn *et al.*, 2018).

The average lesion size (Table VII) on the PAN for *n* measured 5.4 mm × 5.6 mm in its maximum vertical and horizontal dimensions. Similar findings were reported by Ramis-Alario *et al* (2019) where averages measured 5.04 mm vertically and an area of 36.37 mm<sup>2</sup> for AP lesions in general. The current study's CBCT measurement average was 4.9 mm × 4.8 mm × 5.6 mm. Ramis-Alario *et al* (2019) reported 6.36 mm with a surface area of 44.76 mm<sup>2</sup> in the coronal and 6.38 mm with a surface area of 36.59 mm<sup>2</sup> in the sagittal sections respectively. Relatively similar findings between these two studies when comparing perforating to non-specific AP lesions may be coincidental or suggest no correlation between lesion size and perforation. Although further investigation necessitates this hypothesis.

Diagnostic accuracy studies can be very helpful in evaluating the worth of a specific test. Although it is well known that these types of studies can be misleading. Risking bias through methodological deficiencies: sampling, data collection, interpretation and execution. Attempts to increase transparency and complete reporting of diagnostic accuracy studies have been suggested, most notably the Standards for Reporting Diagnostic Accuracy Studies (STARD) initiative. Inspired by the Consolidated Standards for the Reporting of Trials (CONSORT) for the reporting of randomised control trials, STARD was initially released in 2003 and updated in 2015 (Bonita *et al.*, 2006; Cohen *et al.*, 2016). STARD consists of a checklist (Appendix F) of items that should be included when reporting on a diagnostic accuracy study (Anvari *et al.*, 2015; Obuchowski, 2005; Rutjes *et al.*, 2007; Schmidt and Factor, 2013). In 2019 it has been shown that there remains a lack of complete and transparent reporting of diagnostic accuracy studies amongst dental journals

(Durkan *et al.*, 2019). It is therefore of importance to acquire the skills to critically appraise the literature with regards to diagnostic accuracy studies. Several benchmark parameters are to be considered during the evaluation of diagnostic accuracy tests. Appraisal of such studies should consider these as a collective and not individual results. Values obtained of sensitivity, specificity, PPV, NPV, diagnostic effectiveness (accuracy), Youden's index, ROC analysis with AUC, LR, and DOR can aid in scrutinising a test (Appendix G). All of whom have strengths and weaknesses (Genders *et al.*, 2012; Johnson and Johnson, 2014; Naeger *et al.*, 2013; Parikh *et al.*, 2008; Sauerbrei and Blettner, 2009).

The 3D nature of CBCT appears to be far more superior compared to conventional modalities such as periapical radiographs and pantomography with regards to apical lesion detection. The risk of FN results may, therefore, be greater when 2D radiographic modalities are used. The use of CBCT as a diagnostic tool in detecting apical pathology has its own limitations especially the relatively high effective dose (Fuji *et al.*, 2016; Persoon and Özok, 2017). Employing CBCT as a diagnostic tool should be reserved for selected cases. Adherence to the as low as reasonably achievable (ALARA) principle, SEDENTEXCT basic principles, and radiation protection protocols is of great importance (EADMFR, 2011). In such cases, a small FOV is recommended ranging from a single tooth at the ROI to a couple of teeth. CBCT was established as the 'reference standard' with a known near 100% detection of apical radiolucencies (Dutra *et al.*, 2016; Ramis-Alario *et al.*, 2019). With intra- and inter-observer agreement shown to be 'substantial' amongst both modalities. This study relates to the same trend in detecting apical lesion 'perforation' of the maxillary sinus floor when compared to non-specific apical radiolucencies. With a CI of 95%, CBCT has shown: 100% sensitivity, specificity, PPV, NPV, and diagnostic effectiveness (accuracy). With Youden's index at 1.000, an AUC of 1.000, LR+ to  $\infty$ , and LR- of 0.00. Presenting the impression of near-perfect detection of apical lesions perforating the maxillary sinus floor.

Accuracy studies regarding PAN and apical lesion detection are limited in the literature. A diagnostic accuracy study by Nardi *et al* (2017) where CBCT versus PAN regarding AP detection in teeth 'without' RCT reported results of PAN: 34.2% sensitivity, 95.8% specificity, 89.1% PPV, 59.3% NPV, and 65.0% diagnostic effectiveness (accuracy). Another accuracy study by Nardi *et al* (2018) where CBCT versus PAN regarding AP detection in RCT'd teeth with asymptomatic AP

reported results of PAN: 48.8% sensitivity, 93.8% specificity, 88.6% PPV, 64.7% NPV, and 71.3% diagnostic effectiveness (accuracy). Other studies regarding AP detection on PANs reported a sensitivity of 28% and 82% respectively (Ramis-Alario *et al.*, 2019). The latter depicts considerable discrepancy where factors; such as tooth condition, patient age range, systemic conditions, and geographic location may be explanatory. An accuracy study by Ramis-Alario *et al* (2019) regarding apical area measurements in CBCT versus PAN versus periapical radiographs concluded that failure rate in detecting AP in posterior teeth is three times higher than in anterior teeth. Nardi *et al* (2018) concluded that the lowest detection rate of AP was in the maxillary/mandibular incisors, and the upper molars. The current study showed PAN: 14.286% sensitivity, 79.910% specificity, 6.316% PPV, 90.769% NPV, and 74.227% diagnostic effectiveness (accuracy) (Figure 7). The outcome of diagnostic effectiveness (accuracy) in the current study's setting is of limited value. It is not considered an intrinsic property of a test and will remain high where disease prevalence is low. When two tests in the same population are compared these may have different sensitivities, specificities, FP, and FN results. It is therefore suggested to consider the values of sensitivity and specificity as independent entities. Youden's index scored 0.05805. Considered a summarized representation of a test's performance with a value range of 0 to 1 with 0 being 'very poor'. Scoring an AUC of 0.529, whereby 0.5 is to be considered the lower limit. Indicating that the test's ability to discriminate between subjects with or without disease as 'bad'. LR+ is how likely a test would be positive in diseased subjects where LR+ greater than 10 is considered as 'convincing' evidence. LR- is how likely a test would be negative in non-diseased subjects where LR- less than 0.1 is considered as 'convincing' evidence. When both probabilities equal to 1 a test is of no value. The PAN scored an LR+ of 1.07 and LR- of 0.71 (Figure 10). Indicative of 'poor' ability in ruling in or ruling out disease (Anvari *et al.*, 2015; Fischer *et al.*, 2003).

Comparative tests of the modalities; included a comparison ROC curve analysis showing a difference in AUC of 0.471, z-statistic result of 10.447, and significance level of  $P < 0.0001$  (Figure 12). DOR calculation was 0.6629 indicating 'poor' usefulness. DOR shows a general estimation of discriminative power where a result greater than 1 would consider a test 'useful' (Figure 14). McNemar's test to assess the difference between the paired proportions resulted in  $P < 0.0001$  (Figure 15). Indicating a significant difference amongst the two proportions with the observed

findings being unlikely due to chance. Thereby rejecting  $H_0$  and accepting  $H_1$  (Anvari *et al.*, 2015; Fischer *et al.*, 2003; Hanley and McNeil, 1982; Park *et al.*, 2004; Zweig and Campbell, 1993).

The overall performance of the PAN for the investigated entity appears ‘poor’ and insufficient as a diagnostic tool. The current study showed a relatively similar trend compared to previous papers. Albeit keeping in mind the study was conducted only on posterior teeth and detection of subsequent ‘perforation’. The task of identifying such pathology is to be considered more diagnostically challenging than merely apical lesion detection.





## 6.1. Case examples

### 6.1.1. Case 1

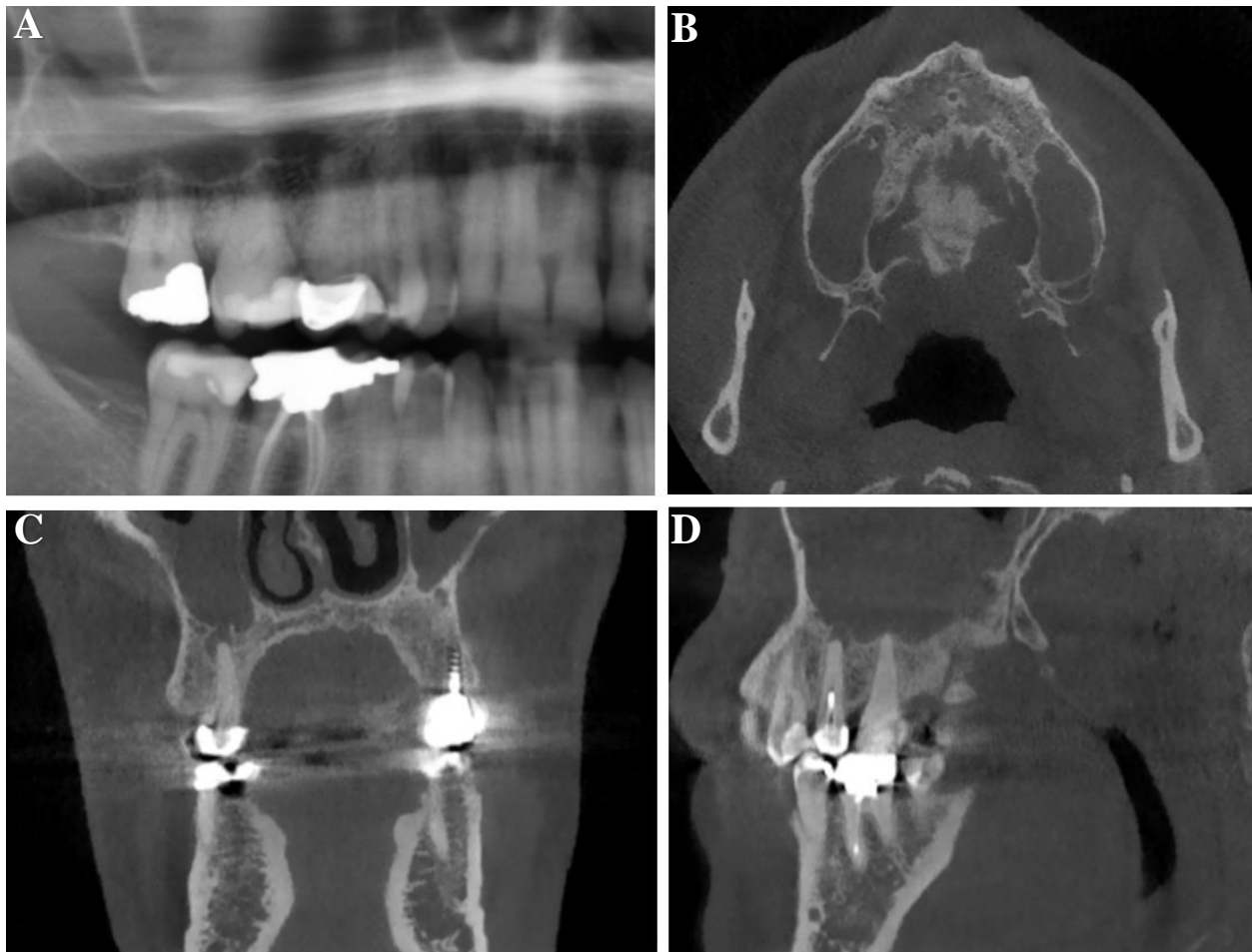


**Figure 16.** ROI tooth 15. **A**, cropped PAN depicting a well-defined, corticated, periapical radiolucency at restored tooth 15 causing elevation of the maxillary sinus floor. Partial opacification of the maxillary sinus is observed. CBCT slices: **B**, axial, **C**, coronal, and **D**, sagittal view. Showing a well-defined periapical low-density with breaching of the maxillary sinus floor. Mucosal reaction in the right maxillary sinus can be observed.

### 6.1.2. Case 2

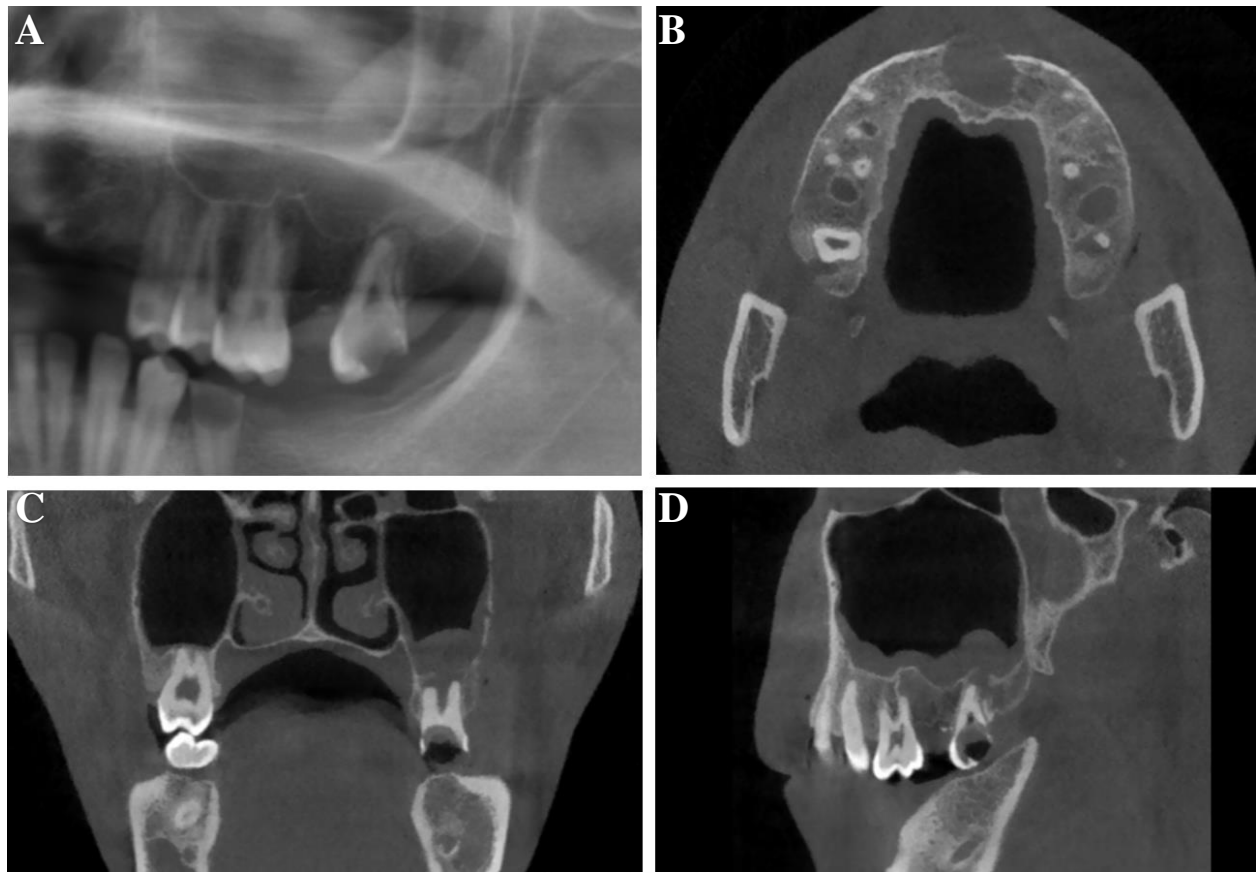


**Figure 17.** ROI tooth 28. **A**, cropped PAN depicting a well-defined, corticated, periapical radiolucency at carious tooth 28 causing elevation of the maxillary sinus floor. Partial opacification of the maxillary sinus is observed. CBCT slices: **B**, axial, **C**, coronal, and **D**, sagittal view. Showing a well-defined periapical low-density with breaching of the maxillary sinus floor. Mucosal reaction in the left maxillary sinus can be observed.

### 6.1.3. Case 3

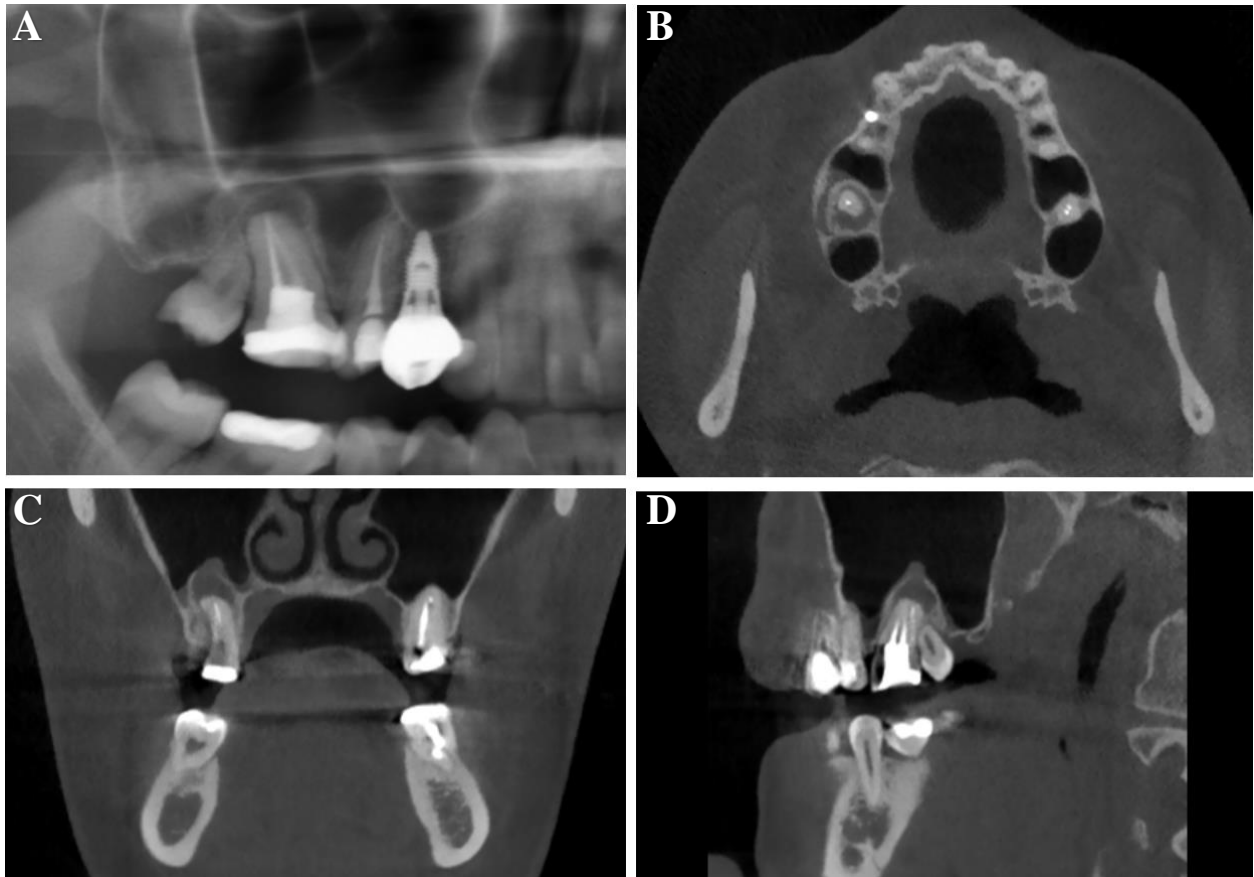


**Figure 18.** ROI tooth 17. **A**, cropped PAN depicting a well-defined, corticated, periapical radiolucency at endodontically treated tooth 17 causing elevation of the maxillary sinus floor and discontinuation of the bony margins of the lesion at the superior border. CBCT slices: **B**, axial, **C**, coronal, and **D**, sagittal view. Showing a well-defined periapical low-density with elevation and breaching of the maxillary sinus floor.

#### 6.1.4. Case 4

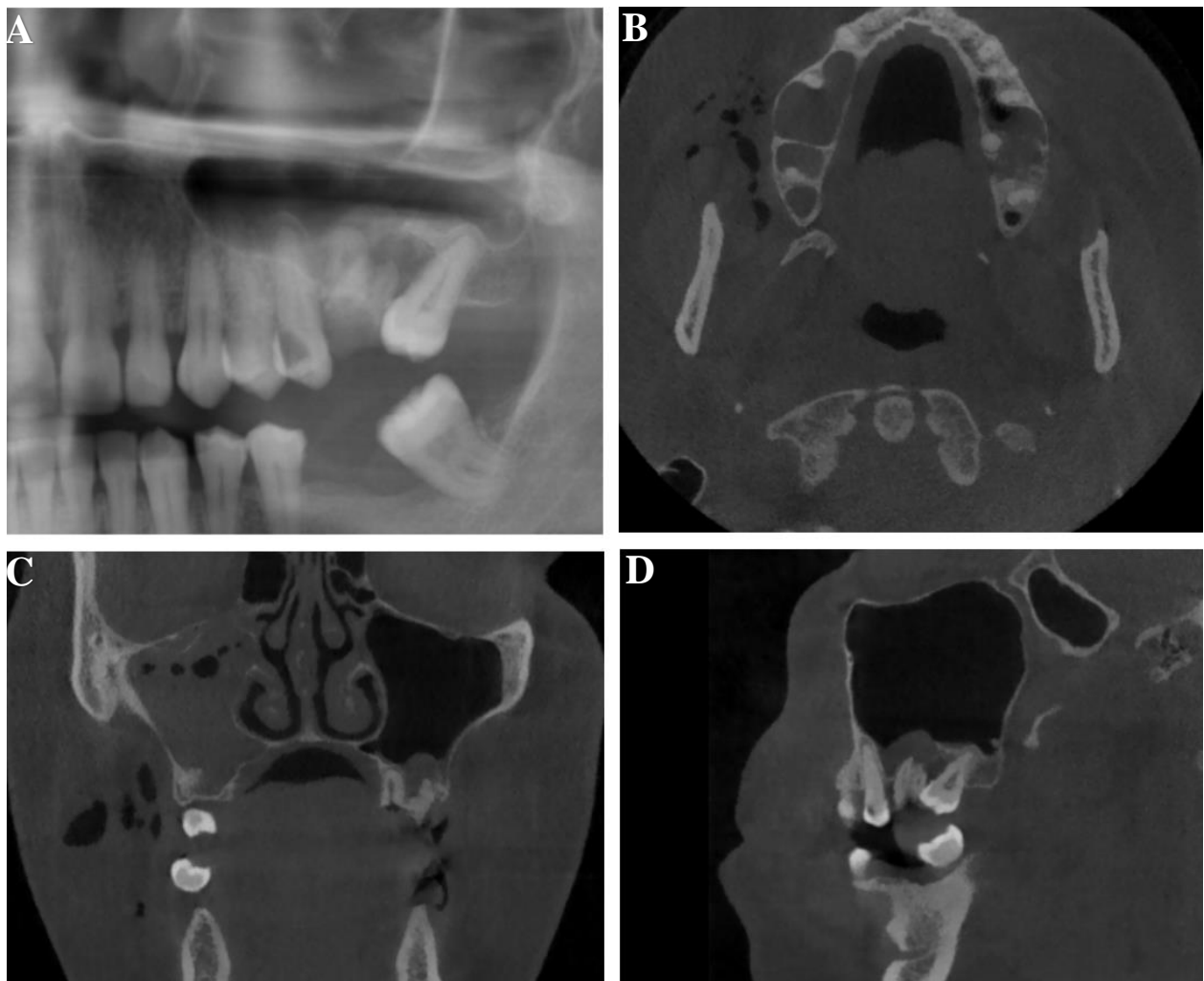


**Figure 19.** ROI tooth 26. **A**, cropped PAN depicting a well-defined, uncorticated, periapical radiolucency at carious tooth 26 causing elevation of the maxillary sinus floor and discontinuation of the bony margins of the lesion at the superior border. CBCT slices: **B**, axial, **C**, coronal, and **D**, sagittal view. Showing a periapical low-density with elevation and discontinuation of the maxillary sinus floor. Mucosal reaction in the left maxillary sinus is observed.

### 6.1.5. Case 5

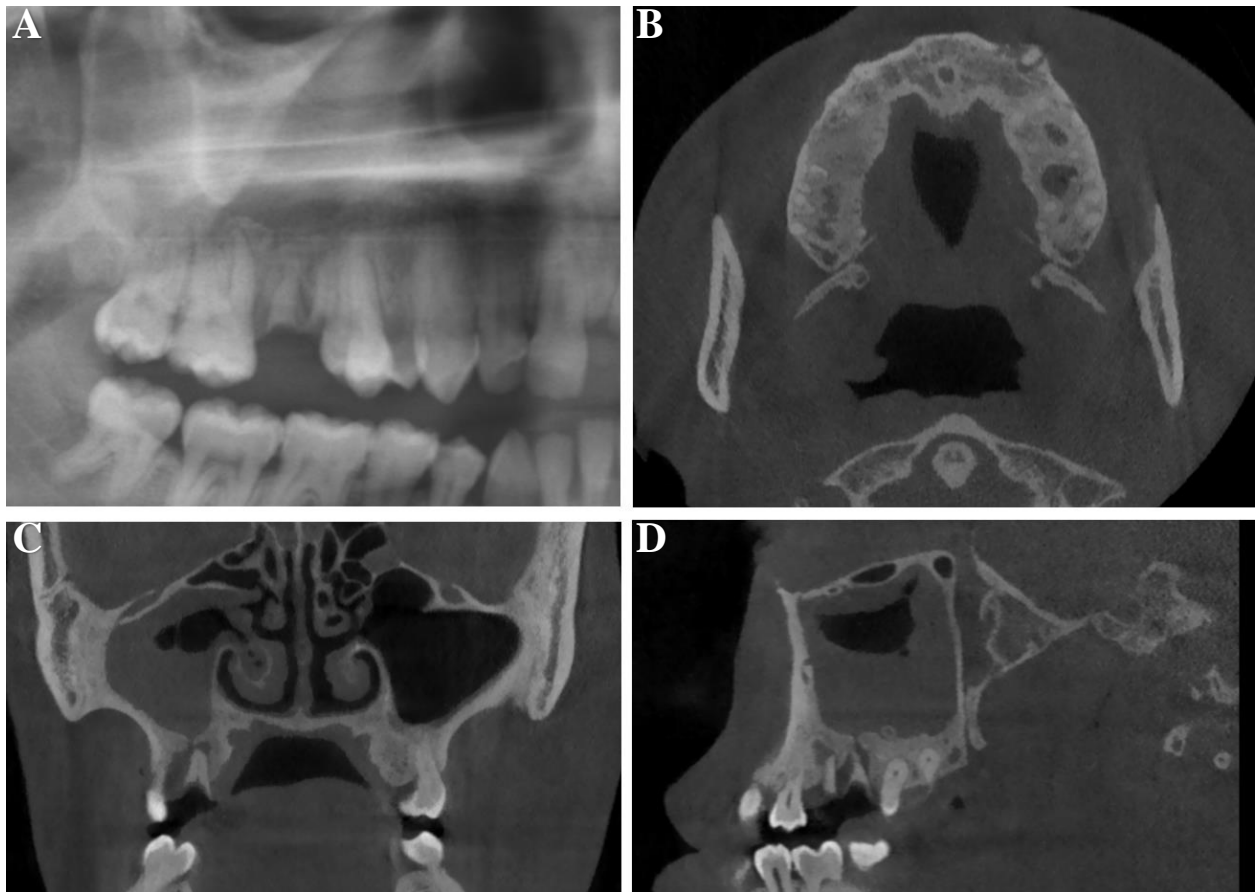


**Figure 20.** ROI tooth 16. **A**, cropped PAN depicting an ill-defined periapical radiolucency at the root rests of tooth 16. Partial opacification of the right maxillary sinus is observed. CBCT slices: **B**, axial, **C**, coronal, and **D**, sagittal view. Showing a well-defined periapical low-density with breaching of the maxillary sinus floor and adjacent osteosclerosis. Mucosal reaction in the right maxillary sinus is observed.

## CHAPTER 7: CONCLUSION

The  $H_0$  that PAN, when compared to CBCT, has equal diagnostic accuracy regarding detection of apical lesions perforating the maxillary sinus floor has been rejected. The PAN demonstrated 'poor' diagnostic capabilities in almost all criteria in this study.

Where 42 cases of maxillary sinus floor perforation of odontogenic origin were analysed. Prevalence corresponded to 8.66% i.e. a ratio of 1 tooth in every 11 with apical lesions presented with maxillary floor perforation. The median and average age showed prevalence for the 4<sup>th</sup> decade with a negligible gender ratio. The majority of cases associated the 1<sup>st</sup> molar with slight 2<sup>nd</sup> quadrant predominance. A great number of lesions presented asymptomatic. Predominant radiographic features included well-defined lucent/low-densities. High rates of the associated teeth were previously restored or RCT'd. Almost all cases depicted maxillary sinus mucosal reaction.

It is suggested that if clinical examination, testing, and conventional imaging present inconclusive further investigation of a suspicious tooth may necessitate. In selected cases, small FOV CBCT accompanied by appropriate interpretation and reporting thereof by a skilled clinician may be considered. The ALARA principle, SEDENTEXCT basic principles, and radiation protection protocols should be adhered to when considering further investigation by advanced imaging such as CBCT. Clinical judgement needs to be justified by equating the overall costs to benefits. This may aid in subsequent correct diagnosis and treatment planning thereby facilitating in achieving an uncomplicated outcome (Dutra *et al.*, 2016; EADMFR, 2018; Holroyd and Gulson, 2009; Tataryn *et al.*, 2018).

## CHAPTER 8: LIMITATIONS AND RECOMMENDATIONS

The current study is at risk of bias due to particular aspects of the methodology. There were only two observers with the primary observer being the same individual who collected the data. To prevent a systematic difference in the observed measurement from the true value. It would be beneficial to calculate the ideal number of observers and subjects per observer needed to decrease bias (Schmidt and Factor, 2013). The reference standard was set by the CBCT modality. In the current setting, this would need to suffice as histological confirmation of lesions are impractical. More than two means of comparison would be preferable. Although alternatives would include a recall basis with the subsequent radiographic examination. The follow-up and exposure for the sole purpose of obtaining data for a study would be unethical.

Fairly strict criteria limited the number of subjects available. At the site where the study was carried out, there was a range of PAN machines. The study limited to a single manufacturer for the purpose of conformity and limiting external variables. Matching PANs from the accrued potentially eligible CBCT subjects scarcely conformed to the criteria. The site is an academic dental hospital that manages large amounts of trauma and extraordinary pathology. The CBCT model used may be considered dated if compared to newer technologies, and the selection of FOV sizes were fairly large with the smallest view including both arches. Larger FOVs have inherent drawbacks such as beam hardening and scatter especially when observing explicit ROIs. This may influence clinician's judgement to risk the amount of exposure. The majority of PANs at the institution are performed by undergraduate dental students, although images being diagnostically acceptable, may not always be optimal.

The use of ROC curve analysis in diagnostic tests statistics are widely applied and considered useful. ROC curves with categorical predictors only have as many thresholds as one less than the category. When the predictor is binary, although considered appropriate, there is only a single threshold. It has been shown that ROC analysis and AUC calculations are inconsistent when using the same univariate binary predictors across several statistical software packages. Alternative means are suggested if results are based on discrete data or at least to present concerns as such when reporting. The use of nominal continuous or quasi-continuous scales for data collection

would be preferable. Should a discrete rating scale be employed the use of a parametric method is recommended. Non-parametric estimation of the AUC tends to underestimate values compared to parametric estimates that have a negligible bias (Bossuyt *et al*, 2013; Muschell, 2019; Park *et al*, 2004). Therefore, a similar study would benefit from implementing measurements of lesion size and degree of perforation.

Review of the literature and to the authors' current knowledge delivered no similar study with regards to apical lesions and maxillary floor perforation. The nearest relatively related references were based on findings of studies on non-specific apical lesion detection and spread of infections. It may be beneficial to revisit the subject.





## REFERENCES

- Abramovitch, K., Rice, D. D., 2014. Basic Principles of Cone Beam Computed Tomography. *Dental Clinics of North America*, 58 (3): 463-484.
- Anvari, A., Halpern, E. F., Samir, A. E., 2015. Statistics 101 for Radiologists. *RadioGraphics*, 35 (6): 1789-1801.
- Blackman, S., 1963. Panoramic Radiography. *British journal of Oral Surgery*, 1 (1): 209-218.
- Boeddinghaus, R., Whyte, A., 2018. Trends in maxillofacial imaging. *Clinical Radiology*, 73 (1): 4-18.
- Bonita, R., Beaglehole, R., Kjellström, T., 2006. *Basic epidemiology*. 2<sup>nd</sup> Edition. Switzerland: World Health Organization.
- Bornstein, M. M., Wasmer, J., Sendi, P., Janner, S. F. M., Buser, D., von Arx, T., 2012. Characteristics and Dimensions of the Schneiderian Membrane and Apical Bone in Maxillary Molars Referred for Apical Surgery: A Comparative Radiographic Analysis Using Limited Cone Beam Computed Tomography. *Journal of Endodontics*, 38 (1): 51-57.
- Bossuyt, P., Davenport, C., Deeks, J., Hyde, C., Leeflang, M., Scholten, R., 2013. Interpreting results and drawing conclusions. In: Deeks, J. J., Bossuyt, P. M., Gatsonis, C., *Cochrane Handbook for Systematic Reviews of Diagnostic Test Accuracy Version 0.9*. The Cochrane Collaboration. Available from: <http://srdta.cochrane.org/>. Last accessed: 15<sup>th</sup> Dec 2020.
- Cawson, R. A., Odell, E. W., 2008. *Cawson's Essentials of Oral Pathology and Oral Medicine*. 8<sup>th</sup> Edition. UK: Churchill Livingstone.

Chapman, M. N., Nadgir, R. N., Akman, A. S., Saito, N., Sekiya, K., Kaneda, T., Sakai, O., 2013. Periapical Lucency around the Tooth: Radiologic Evaluation and Differential Diagnosis. *RadioGraphics*, 33 (1): E15-E32.

Cohen, J. F., Korevaar, D. A., Altman, D. G., Bruns, D. E., Gatsonis, C. A., Hooft, L., Irwig, L., Levine, D., Reitsma, J. B., de Vet, H. C. W., Bossuyt, P. M. M., 2016. STARD 2015 guidelines for reporting diagnostic accuracy studies: explanation and elaboration. *British Medical Journal Open* 2016;6:e012799. doi: 10.1136/bmjopen-2016-012799.

Constantine, S., Clark, B., Kiermeier, A., Anderson, P., 2019. Panoramic radiography is of limited value in the evaluation of maxillary sinus disease. *Oral Surgery, Oral Medicine, Oral Pathology and Oral Radiology*, 127 (3): 237-245.

Cordero, G. B., Ferrer, S. M., Fernández, L., 2015. Odontogenic Sinusitis, Oro-antral Fistula and Surgical Repair by Bichat's Fat Pad: Literature Review. *Acta Otorrinolaringológica Española*, 67 (2): 107-113.

Devlin, H., Yuan, J., 2013. Object position and image magnification in dental panoramic radiography: a theoretical analysis. *Dentomaxillofacial Radiology*, 42(1): 29951683. doi: 10.1259/dmfr/29951683.

Drake, R., Mitchell, A. W. M., Vogl, A. W., 2014. *Gray's Anatomy for Students*. 3<sup>rd</sup> Edition. Philadelphia: Churchill Livingstone.

Drumond, J. P., Allegro, B. B., Novo, N. F., de Miranda, S. L., Sendyk, W. R., 2017. Evaluation of the Prevalence of Maxillary Sinuses Abnormalities through Spiral Computed Tomography (CT). *International Archives of Otorhinolaryngology*. 21 (2): 126-133. doi: 10.1055/s-0036-1593834.

Durkan, M., Chauhan, R., Pandis, N., Cobourne, M. T., Seehra, J., 2019. Adequate Reporting of Dental Accuracy Studies is Lacking: An Assessment of Reporting in Relation to the Standards for

Reporting of Diagnostic Accuracy Studies Statement. *The Journal of Evidence-Based Dental Practice*, 19 (3): 283-294.

Dutra, K. L., Haas, L., Porporatti, A. L., Flores-Mir, C., Santos, J. N., Mezzomo, L. A., Corrêa, M., Canto, G. D. L., 2016. Diagnostic Accuracy of Cone-beam Computed Tomography and Conventional Radiography on Apical Periodontitis: A Systematic Review and Meta-analysis. *Journal of Endodontics*, 42 (3): 356-364.

European Academy of DentoMaxilloFacial Radiology., 2011. Basic Principles for Use of Dental Cone Beam CT. Available from: <http://www.sedentexct.eu/content/basic-principles-use-dental-cone-beam-ct>. Last accessed: 26<sup>th</sup> Aug 2018.

Farman, A. G., Nortjé, C. J., Wood, R. E., 1993. *Oral and Maxillofacial Diagnostic Imaging*. St Louis, Missouri: Mosby.

Fischer, J. E., Bachmann, L. M., Jaeschke, R., 2003. A readers' guide to the interpretation of diagnostic test properties: clinical example of sepsis. *Intensive Care Medicine*, 29 (7): 1043-1051.

Fuji, R., Suehara, M., Sekiya, S., Miyayoshi, N., Asai, T., Morinaga, K., Muramatsu, T., Furusawa, M., 2016. CBCT-based Diagnosis of Periapical Lesion of Maxillary First Premolar Mimicking That of Second Premolar. *The Bulletin of Tokyo Dental College*, 57 (4): 291-297.

Genders, T. S. S., Spronk, S., Stijnen, T., Steyerberg, E. W., Lesaffre, E., Hunink, M. G. M., 2012. Methods for Calculating Sensitivity and Specificity of Clustered Data: A Tutorial. *Radiology*, 265 (3): 910-916.

Guerra-Pereira, I., Vaz, P., Faria-Almeida, R., Braga, A. C., Felino, A., 2015. CT maxillary sinus evaluation--A retrospective cohort study. *Medicina Oral Patologia Oral y Cirugia Bucal*. 20 (4): e419-e426.

Hallikainen, D., 1996. History of Panoramic Radiography. *Acta Radiologica*, 37 (2): 441-445.

Hanley, J. A., McNeil, B. J., 1982. The meaning and use of the area under a receiver operating characteristic (ROC) curve. *Radiology*, 143 (1): 29-36.

Hol, C., Hellén-Halme, K., Torgersen, G., Nilsson, M., Møystad, A., 2015. How do dentists use CBCT in dental clinics? A Norwegian nationwide survey. *Acta Odontologica Scandinavica*, 73 (3): 195-201.

Holroyd, J. R., Gulson, A. D., 2009. The Radiation Protection Implications of the Use of Cone Beam Computed Tomography (CBCT) in Dentistry - What You Need To Know. Available from: [http://www.sedentexct.eu/system/files/sedentexct\\_project\\_guidance\\_uk.pdf](http://www.sedentexct.eu/system/files/sedentexct_project_guidance_uk.pdf). Last accessed: 26<sup>th</sup> Aug 2018.

Horner, K., O'Malley, L., Taylor, K., Glenny, A. M., 2015. Guidelines for clinical use of CBCT: a review. *Dentomaxillofacial Radiology*, 44 (1): 20140225. doi: 10.1259/dmfr.20140225.

Hussein, F. E., Liew, A. K. C., Ramlee, R. A., Abdullah, D., Chong, B. S., 2016. Factors Associated with Apical Periodontitis: A Multilevel Analysis. *Journal of Endodontics*, 42 (10): 1441-1445.

Jaul, E. and Barron, J., 2017. Age-Related Diseases and Clinical and Public Health Implications for the 85 Years Old and Over Population. *Frontiers in Public Health*, 11 (5): 335. doi: 10.3389/fpubh.2017.00335.

Johnson, K. M., Johnson, B. K., 2014. Visual Presentation of Statistical Concepts in Diagnostic Testing: The 2 × 2 diagram. *American Journal of Roentgenology*, 203 (1): W14 – W20.

Kamburoğlu, K., Yulmaz, F., Gulsahi, K., Gulen, O., Gulsahi, A., 2017. Change in Periapical Lesion and Adjacent Mucosal Thickening Dimensions One Year after Endodontic Treatment: Volumetric Cone-beam Computed Tomography Assessment. *Journal of Endodontics*, 43 (2): 218-224.

Kantor, M. L., Slome, B. A., 1989. Efficacy of Panoramic Radiography in Dental Diagnosis and Treatment Planning. *Journal of Dental Research*, 68 (5): 810-812.

Karabucak, B., Bunes., A., Chehoud, C., Kohli, M. R., Setzer, F., 2016. Prevalence of Apical Periodontitis in Endodontically Treated Premolars and Molars with Untreated Canal: A Cone-beam Computed Tomography Study. *Journal of Endodontics*, 42 (4): 538-541.

Kiljunen, T., Kaasalainen, T., Suomalainen, A., Kortensniem, M., 2015. Dental cone beam CT: A review. *Physica Medica*, 31 (8): 844-860.

Kumar, M., Shanavas, M., Sidappa, A., Kiran, M., 2014. Cone Beam Computed Tomography – Know its Secrets. *Journal of International Oral Health*, 7 (2): 64-68.

Laney, W. R., Tolman, D. E., 1968. 'The use of panoramic radiography in the medical centre', paper presented at the American Academy of Oral Roentgenology's 2<sup>nd</sup> annual seminar on panoramic radiography, Chicago, Illinois, 4 February.

Lee, G. S., Kim, J. S., Seo, Y. S, Kim, J. D., 2013. Effective dose from direct and indirect digital panoramic units. *Imaging Science in Dentistry*, 43 (2): 77-84.

Lim, L. Z., Padilla, R. J., Reside, G. J., Tyndall, D. A., 2018. Comparing panoramic radiographs and CBCT: Impact on radiographic features and differential diagnoses. *Oral Surgery, Oral Medicine, Oral Pathology and Oral Radiology*, 126 (1): 63-71.

Lofthag-Hansen, S., Huumonen, S., Gröndahl, K., Gröndahl, H. G., 2007. Limited cone-beam CT and intra-oral radiography for the diagnosis of periapical pathology. *Oral Surgery, Oral Medicine, Oral Pathology, Oral Radiology, and Endodontology*, 103 (1): 114-119.

Lopes, L. J., Gamba, T. O., Bertinato, J. V. J., Freitas, D. Q., 2016. Comparison of panoramic radiography and CBCT to identify maxillary posterior roots invading the maxillary sinus. *Dentomaxillofacial Radiology*, 45 (6): 20160043. doi: 10.1259/dmfr.20160043.

Lozano-Carrascal, N., Salomó-Coll, O., Gehrke, S. A., Calvo-Guirado, J. L, Hernández-Alfaro, F., Gargallo-Albiol, J., 2017. Radiological evaluation of maxillary sinus anatomy: A cross-sectional study of 300 patients. *Annals of Anatomy*, 214 (2017): 1-8.

Matzen, L. H, Schropp, L., Spin-Neto, R., Wenzel, A., 2016. Radiographic signs of pathology determining removal of an impacted mandibular third molar assessed in a panoramic image or CBCT. *Dentomaxillofacial Radiology*, 46 (1): 20160330. doi: 10.1259/dmfr.20160330.

Mckenna, G. and Burke, F. M., 2010. Age-related oral changes. *Dental Update Publication*, 37 (8): 519-23.

Mohamed, N. and Barnes, 2018. Early childhood caries and dental treatment need in low socio-economic communities in Cape Town, South Africa. *Health SA Gesondheid*, 23 (0): a1039. doi: 10.4102/hsag.v23i0.1039.

Murray, D., Whyte, A., 2002. Dental Tomography: What the general Radiologist Needs to Know. *Clinical Radiology*, 57 (1): 1-7.

Muschelli, J., 2019. ROC and AUC with a Binary Predictor: a Potentially Misleading Metric. *Journal of Classification*. doi: 10.1007/s00357-019-09345-1.

Naeger, D. M., Kohi, M. P., Webb, E. M., Phelps, A., Ordovas, K. G., Newman, T. B., 2013. Correctly Using Sensitivity, Specificity, and Predictive Values in Clinical Practice: How to Avoid Three Common Pitfalls. *American Journal of Roentgenology*, 200 (6): W566 – W570.

Nardi, C., Calistri, L., Grazzini, G., Desideri, I., Lorini, C., Occhipinti, M., Mungai, F., Colagrande, S., 2018. Is Panoramic Radiography an Accurate Imaging Technique for the Detection of Endodontically Treated Asymptomatic Apical Periodontitis? *Journal of Endodontics*, 44 (10): 1500-1508.

Nardi, C., Calistri, L., Pradella, S., Desideri, I., Lorini, C., Colagrande, S., 2017. Accuracy of Orthopantomography for Apical Periodontitis without Endodontic Treatment. *Journal of Endodontics*, 43 (10): 1640-1646.

Neville, B. W., Allen, C. M., Damm, D. D., Chi, A. C., 2016. *Oral and Maxillofacial Pathology*. 4<sup>th</sup> Edition. St Louis, Missouri: Elsevier.

Noffke, C. E. E., Farman, A. G., Nel, S., Nzima, N., 2011. Guidelines for safe use of dental and maxillofacial CBCT: a review with recommendations for South Africa. *South African Dental Journal*, 66 (6): 262-266.

Obayashi, N., Ariji, Y., Goto, M., Izumi, M., Naitoh, M., Kurita, K., Shimozato, K., Ariji, E., 2004. Spread of odontogenic infection originating in the maxillary teeth: Computerized tomographic assessment. *Oral Surgery, Oral Medicine, Oral Pathology, Oral Radiology, and Endodontology*, 98 (2): 223-231.

Obuchowski, N. A., 2005. Fundamentals of Clinical Research for Radiologists. *American Journal of Roentgenology*, 184 (2): 364-372.

Parikh, R., Mathai, A., Parikh, S., Sekhar, G. C., Thomas, R., 2008. Understanding and using sensitivity, specificity and predictive values. *Indian Journal of Ophthalmology*, 56 (1): 45-50.

Park, S. H., Goo, J. M., Jo, C. H., 2004. Receiver operating characteristic (ROC) curve: practical review for radiologists. *Korean Journal of Radiology*, 5 (1): 11-18.

Pauwels, R., Araki, K., Siewerdsen, J. H., Thongvigitmanee, S. S., 2015. Technical aspects of dental CBCT: state of the art. *Dentomaxillofacial Radiology*, 44 (1): 20140224. doi: 10.1259/dmfr.20140224.

Persoon., I. F., Özok, A. R., 2017. Definitions and Epidemiology of Endodontic Infections. *Current Oral Health Reports*, 4 (4): 278-285.

Ramis-Alario, A., Tarazona-Alvarez, B., Cervera-Ballester, J., Soto-Peñaloza, D., Peñarrocha-Diago, M., Peñarrocha-Oltra, Peñarrocha-Diago, M., 2019. Comparison of diagnostic accuracy between periapical and panoramic radiographs and cone beam computed tomography in measuring the periapical area of teeth scheduled for periapical surgery. A cross-sectional study. *Journal of Clinical and Experimental Dentistry*, 11 (8): e732-e738.

Rocha, F. F., Batista, J. D., Silva, C. J., Júnior, R. B., Raposo, L. H. A., 2015. Considerations for the Spread of Odontogenic Infections – Diagnosis and Treatment. *In: M. H. K. Motamedi, ed. A Textbook of Advanced Oral and Maxillofacial Surgery Volume 2*, Rijeka, Croatia. InTech: 341-358.

Roque-Torres, G. D., Ramirez-Sotelo, L. R., de Azevedo Vaz, S. L., de Almeida de Bóscolo, S. M., Bóscolo, F. N., 2015. Association between maxillary sinus pathologies and healthy teeth. *Brazilian Journal of Otorhinolaryngology*, 82 (1): 33-38.

Rutjes, A. W. S., Reitsma, J. B., Coomarasamy, A., Khan, K. S., Bossuyt, P. M. M., 2007. Evaluation of Diagnostic tests when there is no gold standard. A review of methods. *Health Technology Assessment*, 11 (50): 1-164.

Santos, O., Pinheiro, L. R., Umetsubo, O. S., Cavalcanti, M. G. P., 2015. CBCT-based evaluation of integrity of cortical sinus close to periapical lesions. *Brazilian Oral Research*, 29 (1): 1-7.

Sauerbrei, W., Blettner, M., 2009. Interpreting Results in 2 × 2 Tables. *Deutsches Ärzteblatt International*, 106 (48): 795-800.

Schmidt, R. L., Factor, R. E., 2013. Understanding Sources of Bias in Diagnostic Accuracy Studies. *Archives of Pathology & Laboratory Medicine*, 137 (4): 558-565.

Shanbhag, S., Karnik, P., Shirkee, P., Shanbhag, V., 2013. Association between Periapical Lesions and Maxillary Sinus Mucosal Thickening: A Retrospective Cone-beam Computed Tomographic Study. *Journal of Endodontics*, 39 (7): 853-857.



Singh, S., 2011. Dental caries rates in South Africa: implications for oral health planning. *Southern Africa Journal of Epidemiology and Infection*, 26 (4): 259-261. doi: 10.1080/10158782.2011.11441463.

Tataryn, R. W., Lewis, M. J., Horalek, A. L., Thompson, C. G., Cha, B. Y., Pokorny, A. T., 2018. Maxillary Sinusitis of Endodontic Origin. Available from: [https://www.aae.org/specialty/wp-content/uploads/sites/2/2018/04/AAE\\_PositionStatement\\_MaxillarySinusitis.pdf](https://www.aae.org/specialty/wp-content/uploads/sites/2/2018/04/AAE_PositionStatement_MaxillarySinusitis.pdf). Last accessed: 26<sup>th</sup> Aug 2018.

Van der Veken, D., Curvers, F., Fieuws S., Lambrechts, P., 2017. Prevalence of apical periodontitis and root filled teeth in a Belgian subpopulation found on CBCT images. *International Endodontic Journal*, 50 (4): 317-329.

Venskutonis, T., Plotino, G., Juodzbaly, G., Mickevičienė, L., 2014. The Importance of Cone-beam Computed Tomography in the Management of Endodontic Problems: A Review of the Literature. *Journal of Endodontics*, 40 (12): 1895-1901.

Zirk, M., Dreiseidler, T., Pohl, M., Rothamel, D., Buller, J., Peters, F., Zöller, J. E., Kreppel, M., 2017. Odontogenic sinusitis maxillaris: A retrospective study of 121 cases with surgical intervention. *Journal of Cranio-Maxillo-Facial Surgery*, 45 (4): 520-525.

Zweig, M. H., Campbell, G., 1993. Receiver-operating characteristic (ROC) plots: a fundamental evaluation tool in clinical medicine. *Clinical Chemistry*, 39 (8): 561-577.

## APPENDICES

### Appendix A: Eligible participants form

<b>Record no.</b>	<b>Gender (Male/Female)</b>	<b>Age (Years)</b>	<b>Main complaint/purpose for CBCT acquisition</b>	<b>CBCT (available and eligible mark with a ✓ )</b>	<b>PAN (available and eligible mark with a ✓ )</b>

## Appendix B: Radiographic assessment form

Record no.: . . . . . PAN/CBCT

<b>Maxillary posterior teeth periapical pathology</b>	
( 1 ) present ( 2 ) absent	
If present:	
Tooth no.: . . . . .	
<b>Maxillary sinus floor bony changes</b>	
( 1 ) present ( 2 ) absent	
If present:	
Perforation: ( 1 ) present ( 2 ) absent	
Lesion effect: ( 1 ) solely perforation ( 2 ) elevation and perforation	
<b>Lesion analysis</b>	
Radiographic appearance PAN/CBCT respectively: ( 1 ) lucent/low-density ( 2 ) mixed/intermediate-density ( 3 ) opaque/high-density	
Margins of lesion: ( 1 ) well-defined/smooth ( 2 ) ill-defined/irregular	
Greatest dimensions in millimetres: PAN: . . . . . × . . . . . CBCT: . . . . . × . . . . . × . . . . .	
<b>Associated tooth analysis</b>	
Tooth condition: ( 1 ) sound ( 2 ) carious ( 3 ) restored ( 4 ) endodontically treated ( 5 ) surgically treated	
Lesion effect: ( 1 ) tooth displaced ( 2 ) tooth elevated ( 3 ) none	
<b>Maxillary sinus mucosal lining changes</b>	
( 1 ) present ( 2 ) absent	
If present:	
( 1 ) mucositis ( 2 ) polyp/mucous retention pseudo cyst ( 3 ) mucocele	
Greatest dimensions in millimetres: PAN: . . . . . × . . . . . CBCT: . . . . . × . . . . . × . . . . .	
<b>Maxillary sinus opacification (PAN)</b>	
( 1 ) complete ( 2 ) partial ( 3 ) none	
<b>Maxillary sinus content (CBCT)</b>	
( 1 ) fluid filled ( 2 ) none	

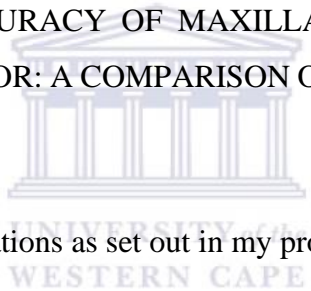
**Appendix C: Letter requesting permission to view radiographic records**

Re: Request permission for use of radiographic records from the Department of Diagnostics and Radiology, Faculty of Dentistry, University of the Western Cape, Tygerberg.

Dear Mr/Ms

I hereby request permission from the principal administrator to make use of records of previously performed pantomographs (PAN) and cone-beam computed tomography (CBCT) from the database in the Department of Diagnostics and Radiology, Faculty of Dentistry, University of the Western Cape, Tygerberg. The purpose of this request is for data collection which pertains in part of my research required for fulfilling my MSc thesis in Maxillofacial Radiology.


Thesis topic: DIAGNOSTIC ACCURACY OF MAXILLARY PERIAPICAL PATHOLOGY PERFORATING THE SINUS FLOOR: A COMPARISON OF PANTOMOGRAPH AND CBCT IMAGES



All ethical considerations and obligations as set out in my protocol will be strictly adhered to. Hope this meets your consideration.

Kind regards.

Jaco Walters

Signed: .....  


April 2019

## Appendix D: Authorization letter to access records



**FACULTY OF DENTISTRY**  
Private Bag X 1, Tygerberg, 7505  
Cape Town, South Africa  
T: +27 937 3110 F: +27 931 2287  
E-mail: sshaik@uwc.ac.za

28 May 2019

To whom it may concern

Re: Permission to use the records from the Department of Radiology

I hereby grant permission to Dr J. Walters to use the records of radiographic images from the Department of Radiology. The purpose is to complete his research that is in partial fulfillment of his M.Sc (Maxillofacial Radiology) degree.

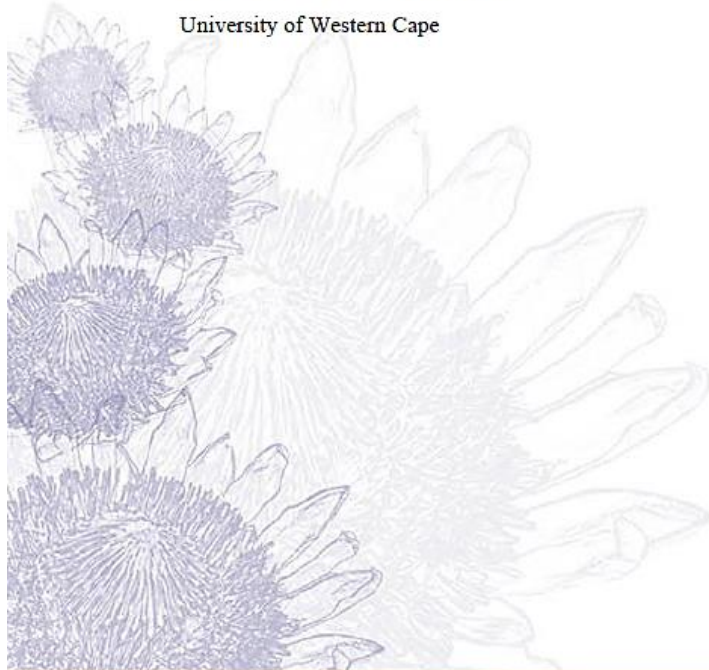
All ethical considerations will be adhered to as set out in his protocol presentation and BMREC application.

Hope this meets your consideration.

Kind regards.

A handwritten signature in black ink, appearing to read "S. Shaik".

Dr Shoayeb Shaik  
HOD – Diagnostics and Radiology  
University of Western Cape



FROM HOPE TO ACTION THROUGH KNOWLEDGE.

## Appendix E: Ethics approval and project registration letter



OFFICE OF THE DIRECTOR: RESEARCH  
RESEARCH AND INNOVATION DIVISION

Private Bag X17, Bellville 7535  
South Africa  
T: +27 21 959 4111/2948  
F: +27 21 959 3170  
E: [research-ethics@uwc.ac.za](mailto:research-ethics@uwc.ac.za)  
[www.uwc.ac.za](http://www.uwc.ac.za)

10 April 2019

Dr J Walters  
Faculty of Dentistry

Ethics Reference Number: BM19/2/5

**Project Title:** Diagnostic accuracy of maxillary periapical pathology perforating the sinus floor: a comparison of pantomograph and CBCT images.

**Approval Period:** 9 April 2019 – 9 April 2020

I hereby certify that the Biomedical Science Research Ethics Committee of the University of the Western Cape approved the scientific methodology and ethics of the above mentioned research project.

Any amendments, extension or other modifications to the protocol must be submitted to the Ethics Committee for approval.

**Please remember to submit a progress report in good time for annual renewal.**

The Committee must be informed of any serious adverse event and/or termination of the study.

A handwritten signature in black ink, appearing to read 'Josias'.

*Ms Patricia Josias  
Research Ethics Committee Officer  
University of the Western Cape*

**BMREC REGISTRATION NUMBER -130416-030**

FROM HOPE TO ACTION THROUGH KNOWLEDGE.

## Appendix F: STARD checklist

Section & Topic	No.	X	Item
<b>TITLE OR ABSTRACT</b>			
	1	X	Identification as a study of diagnostic accuracy using at least one measure of accuracy (such as sensitivity, specificity, predictive values, or AUC)
<b>ABSTRACT</b>			
	2	X	Structured summary of study design, methods, results, and conclusions (for specific guidance, see STARD for Abstracts)
<b>INTRODUCTION</b>			
	3	X	Scientific & clinical background, including the intended use and clinical role of the index test
	4	X	Study objectives and hypotheses
<b>METHODS</b>			
<i>Study design</i>	5	X	Whether data collection was planned before the index test and reference standard were performed (prospective study) or after (retrospective study)
<i>Participants</i>	6	X	Eligibility criteria
	7	X	On what basis potentially eligible participants were identified (such as symptoms, results from previous tests, inclusion in registry)
	8	X	Where and when potentially eligible participants were identified (setting, location and dates)
	9	X	Whether participants formed a consecutive, random or convenience series
<i>Test methods</i>	10a	X	Index test, in sufficient detail to allow replication
	10b	X	Reference standard, in sufficient detail to allow replication
	11	X	Rationale for choosing the reference standard (if alternatives exist)
	12a	X	Definition of and rationale for test positivity cut-offs or result categories of the index test, distinguishing pre-specified from exploratory
	12b	X	Definition of and rationale for test positivity cut-offs or result categories of the reference standard, distinguishing pre-specified from exploratory
	13a	X	Whether clinical information and reference standard results were available to the performers/readers of the index test
	13b	X	Whether clinical information and index test results were available to the assessors of the reference standard
<i>Analysis</i>	14	X	Methods for estimating or comparing measures of diagnostic accuracy
	15	X	How indeterminate index test or reference standard results were handled
	16	X	How missing data on the index test and reference standard were handled
	17	X	Any analyses of variability in diagnostic accuracy, distinguishing pre-specified from exploratory
	18	X	Intended sample size and how it was determined
<b>RESULTS</b>			
<i>Participants</i>	19	X	Flow of participants, using a diagram
	20	X	Baseline demographic and clinical characteristics of participants
	21a	X	Distribution of severity of disease in those with the target condition
	21b	X	Distribution of alternative diagnoses in those without the target condition
	22	X	Time interval and any clinical interventions between index test and reference standard
<i>Test results</i>	23	X	Cross tabulation of the index test results (or their distribution) by the results of the reference standard
	24	X	Estimates of diagnostic accuracy and their precision (such as 95% confidence intervals)
	25	X	Any adverse events from performing the index test or the reference standard
<b>DISCUSSION</b>			
	26	X	Study limitations, including sources of potential bias, statistical uncertainty, and generalizability
	27	X	Implications for practice, including the intended use and clinical role of the index test
<b>OTHER INFORMATION</b>			
	28	X	Registration number and name of registry
	29	X	Where the full study protocol can be accessed
	30	X	Sources of funding and other support; role of funders

## Appendix G: Formulae

**Diagnostic effectiveness (accuracy):**

$$accuracy = \frac{(TP + TN)}{(TP + TN + FP + FN)}$$

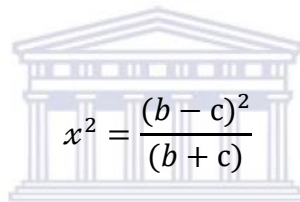
**Diagnostic odds ratio (DOR):**

$$DOR = \left(\frac{TP}{FN}\right) / \left(\frac{FP}{TN}\right)$$

**Likelihood ratio (LR):**

$$LR+ = \frac{sensitivity}{1 - specificity} \quad LR- = \frac{1 - sensitivity}{specificity}$$

**McNemar's test:**



The logo of the University of the Western Cape, featuring a classical building facade with columns and a pediment. The text 'UNIVERSITY of the WESTERN CAPE' is written below the building. The McNemar's test formula is overlaid on the logo.

$$x^2 = \frac{(b - c)^2}{(b + c)}$$

**Negative predictive value (NPV):**

$$NPV = \frac{TN}{(TN + FN)}$$

**Positive predictive value (PPV):**

$$PPV = \frac{TP}{(TP + FP)}$$

**Sensitivity:**

$$sensitivity = \frac{TP}{(TP + FN)}$$

**Specificity:**

$$specificity = \frac{TN}{(TN + FP)}$$



**Youden's index ( $J$ ):**

$$J = \text{sensitivity} + \text{specificity} - 1$$

